On conical horn antennas

Document status and date:
Published: 01/01/1970

Document Version:
Publisher's PDF, also known as Version of Record (includes final page, issue and volume numbers)

Please check the document version of this publication:

• A submitted manuscript is the version of the article upon submission and before peer-review. There can be important differences between the submitted version and the official published version of record. People interested in the research are advised to contact the author for the final version of the publication, or visit the DOI to the publisher's website.
• The final author version and the galley proof are versions of the publication after peer review.
• The final published version features the final layout of the paper including the volume, issue and page numbers.

[Link to publication](#)

ON CONICAL HORN ANTENNAS

by

H.E.M. Koop, J. Dijk   and E.J. Maanders

i

Technische Hogeschool Eindhoven   Eindhoven University of Technology

Eindhoven   Nederland   Eindhoven   The Netherlands

Afdeling Elektrotechniek   Department of Electrical Engineering

On Conical Horn Antennas

by

H.E.M. Koop,   J. Dijk   and E.J. Maanders

Contents.

List of principal symbols.

x, y, z ⎫ ξ, η, ζ ⎭	= cartesian coordinates
ρ, ϕ, z	= cylindrical coordinates
r, θ, ϕ	= spherical coordinates
$\overline{i_r}, \overline{i_\theta}, \overline{i_\phi}$	= unit vectors in spherical coordinates
$\overline{E}$	= electric field vector
$\overline{H}$	= magnetic field vector
$\overline{A}$	= magnetic vector potential
$\overline{F}$	= electric vector potential
ϕ_A, ϕ_F	= scalar potentials
μ	= permeability; order of associated Legendre functions
ε	= permitivity
$k = \dfrac{2\pi}{\lambda} = \omega\sqrt{\mu\varepsilon}$	= wave number medium
ω	= angular frequency of wave
λ	= wavelength
$\kappa = k\sqrt{1 - \beta^2/k^2}$ in a circular waveguide	
$\gamma = \alpha + \beta$	= propagation constant
α	= attenuation constant; top angle cone
β	= phase constant
v_p	= phase velocity
v_g	= group velocity
$B_\nu(z), J_\nu(z), Y_\nu(z), H_\nu(z)$	= solutions to Bessel equation of integer order
$b_\nu(z), j_\nu(z), y_\nu(z), h_\nu(z)$	= solution to Bessel equation of fractional order
$L_\nu^\mu, P_\nu^\mu, Q_\nu^\mu$	= solutions of Legendre functions
ν	= order of Bessel equation; degree of Legendre equation
$h(\mu\phi)$	= harmonic function
$\overline{n}$	= normal vector
$\overline{s} \cdot \overline{S}$	= Poynting vector
χ	= angle of diffraction
$k(\chi)$	= inclination factor

Summary

This report comprises a fundamental study of the near fields
of a conical horn antenna. For this purpose the field components
of the conical horn are deduced from Maxwell's equations.
It appears that it is possible to approximate the aperture
field of a finite conical horn antenna from the fields within
an infinite conical horn.
From the radiating antenna aperture the fields outside the
antenna can be computed and compared with the various measuring
results.
In this way a clearer insight is obtained into the usual
approximations which are related to the flare angle and the
length of the horn.

1. Introduction

Horn antennas are well known as primary radiators for large
parabolic antennas. Recently the conical horn antenna has
become more popular in large reflector antennas owing to
its properties of symmetry. The formulae concerning the
properties of conical horn antennas with relation to their
aperture field are mostly approximations. Most authors
(refs. 14, 15) indicate that the aperture field of a conical
horn antenna is similar to that of a circular waveguide but
with spherical wavefronts. It is further explained that the
approximations are valid if the flare angle of the conical
horn is small and the horn itself long. Mostly, further
information with regard to the length of the horn and the
limitations of the flare angle is not available. It is the
purpose of this paper to investigate the expressions used
and the influence of small flare angles and large apertures.
Therefore, in Section 2 the field equations within the conical
horn are deduced from Maxwell's equations, using electric
and magnetic vector potentials. It is further investigated
what requirements are to be made on the horn parameters in
order   that the aperture field may be represented by fields
of a circular waveguide with spherical wavefronts.
The near field radiation pattern of the horn antenna is
discussed in Section 3 and especially the equation

$$\bar{E}_P = \frac{jk}{4\pi} \iint_S \bar{E}_A \, (1 + \bar{n} \cdot \bar{i}_r) \, \frac{e^{-jkr}}{r} \cdot dS,$$

referred to by several authors (refs. 13, 14, 15), using the
zone construction of Fresnel.
This report comprises part of the graduate work of Koop (ref.19).

2. The aperture field of a conical horn antenna

2.1 Introduction

An antenna is capable of maximum power transfer if the radiation impedance equals that of free space, viz. 120π ohms. In microwave engineering it is common practice to use horn antennas with a diameter much longer than the wavelength. In that case boundary effects may be neglected if the radiation impedance of the antenna equals that of free space.

In this chapter we shall discuss how the dimensions of a conical horn antenna are to be chosen so that it is well matched to free space.

We will also discuss the aperture fields of a conical horn antenna, to see under what conditions the aperture fields can be approximated by the fields of a waveguide with circular cross-section but with spherical wave fronts.

2.2 Vector potentials

In a homogeneous source-free region with the restriction of time dependence to the time factor $e^{j\omega t}$, the field will satisfy the following Maxwell equations:

$$\nabla \times \bar{E} + j\omega\mu\bar{H} = 0 \tag{2.1}$$

$$\nabla \times \bar{H} - j\omega\varepsilon\bar{E} = 0 \tag{2.2}$$

$$\nabla \cdot \bar{E} = 0 \tag{2.3}$$

$$\nabla \cdot \bar{H} = 0 \quad . \tag{2.4}$$

These equations can be solved by introducing vector potentials. Any divergenceless vector is the curl of some other vector; therefore, as $\nabla \cdot \bar{H} = 0$

$$\bar{H} = \nabla \times \bar{A} , \tag{2.5}$$

where $\bar{A}$ is called a magnetic vector potential.

In the same way the electric field $\bar{E}$ can be represented by

$$\bar{E} = - \nabla \times \bar{F} \quad , \tag{2.6}$$

In analogy with $\bar{A}$ the quantity $\bar{F}$ is called the electric vector potential. It is also possible to represent the field by a combination of both vector potentials $\bar{A}$ and $\bar{F}$. Part of the field will be expressed in $\bar{A}$, the remaining part in $\bar{F}$ (ref. 1).

2.2.1. Magnetic vector potential

Substituting Eq. (2.5) in (2.1) we obtain

$$\nabla \times (\bar{E} + j\omega\mu\bar{A}) = 0 \quad . \tag{2.7}$$

Any curl-free vector is the gradient of some vector, hence

$$\bar{E} = - j\omega\mu\bar{A} - \nabla\Phi_A \quad , \tag{2.8}$$

where $\Phi_A = \Phi_A(x,y,z)$ is an arbitrary electric scalar potential. Substituting (2.5) and (2.8) in (2.2) gives

$$\nabla \times \nabla \times \bar{A} - k^2\bar{A} = - j\omega\varepsilon\nabla\Phi_A \quad , \tag{2.9}$$

the frequently encountered parameter $k = \dfrac{2\pi}{\lambda} = \omega\sqrt{\mu\varepsilon}$ and is called the wave number of the medium.
Depending upon the coordinate system used, a value of $\bar{A}$ has been chosen, in such a way that the simplest solution of Eq. (2.9) is obtained. For rectangular coordinates, this equation becomes by a vector identity

$$\nabla(\nabla.\bar{A}) - \Delta\bar{A} - k^2\bar{A} = - j\omega\varepsilon\nabla\Phi_A \quad .$$

For cartesian coordinates the best choice appears to be

$$\nabla.\bar{A} = -j\omega\varepsilon\Phi_A \quad , \tag{2.10}$$

simplifying Eq. (2.9) to

$$\Delta\bar{A} + k^2\bar{A} = 0 \quad . \tag{2.11}$$

This equation is known as the Helmholtz equation or complex wave equation.

2.2.2. Electric vector potential

From Eq. (2.2) and Eq. (2.6) it is readily found that

$$\bar{H} = - j\omega\epsilon\bar{F} - \nabla\Phi_F \ ,$$ (2.12)

where Φ_F is an arbitrary electric potential. If Eq. (2.6) and Eq. (2.12) are now substituted in Eq. (2.1) we obtain

$$\nabla \times \nabla \times \bar{F} - k^2\bar{F} = - j\omega\mu\nabla\Phi_F \ ,$$ (2.13)

being similar to Eq. (2.9).

2.3. The principle of duality

The results obtained in Sec. 2.2 have been collected in Table 2.1 .

Table 2.1.		Table 2.2.	
magnetic vector potential $\bar{A}$	**electric vector potential $\bar{F}$**		
$\bar{H} = \nabla \times \bar{A}$	$\bar{E} = - \nabla \times \bar{F}$	$\bar{A}$	$\bar{F}$
$\nabla \times \bar{H} = j\omega\epsilon\bar{E}$	$-\nabla \times \bar{E} = j\omega\mu\bar{H}$	$\bar{E}$	$\bar{H}$
$-\nabla \times \bar{E} = j\omega\mu\bar{H}$	$\nabla \times \bar{H} = j\omega\epsilon\bar{E}$	$\bar{H}$	$-\bar{E}$
$\nabla.\bar{E} = 0$	$\nabla.\bar{H} = 0$	Φ_A	Φ_F
$\nabla.\bar{H} = 0$	$\nabla.\bar{E} = 0$	ϵ	μ
$\nabla \times \nabla \times \bar{A} - k^2\bar{A} = -j\omega\epsilon\Phi_A$	$\nabla \times \nabla \times \bar{F} - k^2\bar{F} = -j\omega\mu\nabla\Phi_F$	μ	ϵ
$\bar{E}_A = - j\omega\mu\bar{A} - \nabla\Phi_A$	$\bar{H}_F = -j\omega\epsilon\bar{F} - \nabla\Phi_F$	k	k

As will be noticed the equations with electric or magnetic vector potential have the same mathematical form, therefore, their solutions will also have the same mathematical form. In this case they are called dual quantities. In table 2.1., equations for the magnetic vector potential are obtained by systematically interchanging the symbols, in accordance with table 2.2.

It is often convenient to divide a problem into two dual parts. For example, the Maxwell equations can be regarded as a super-position of the equations derived in Sec. 2.2.1 and Sec. 2.2.2; let $\bar{E}_A$ and $\bar{H}_A$ be the fields belonging to $\bar{A}$ and $\bar{E}_F$ and $\bar{H}_F$ the fields belonging to $\bar{F}$, then the following equations are obtained:

$$\bar{E} = \bar{E}_A + \bar{E}_F \qquad\qquad \bar{H} = \bar{H}_A + \bar{H}_F$$

$$\nabla \times \bar{H}_A = j\omega\varepsilon\bar{E}_A \qquad\qquad \nabla \times \bar{E}_A = j\omega\mu\bar{H}_A$$

$$\nabla \times \bar{H}_F = j\omega\varepsilon\bar{E}_F \qquad\qquad -\nabla \times \bar{E}_F = j\omega\mu\bar{H}_F \qquad .$$

The total solution, being the superposition of the two partial solutions, becomes:

$$\bar{E} = -\nabla \times \bar{F} + \frac{1}{j\omega\varepsilon} \nabla \times \nabla \times \bar{A} \qquad\qquad (2.14)$$

$$\bar{H} = \nabla \times \bar{A} + \frac{1}{j\omega\mu} \nabla \times \nabla \times \bar{F} \quad . \qquad\qquad (2.15)$$

Depending upon the purpose we can carry out the calculations in the case of $F \equiv 0$ and $A \neq 0$ or $F \neq 0$ and $A \equiv 0$

2.4.   The vector potential in a spherical coordinate system

Spherical coordinates are most suitable to describe field equations
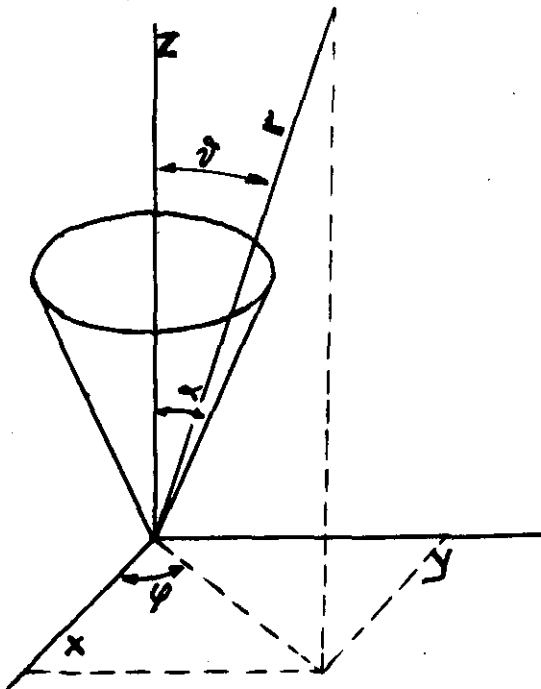
of conical horns and conical waveguides. If we place the apex of a cone in the origin of a spherical coordinate system (Fig. 2.1) and if we use the z-axis as the axis of symmetry, the equation of a cone with a top angle α will be

$$\phi = \alpha \quad . \qquad\qquad (2.16)$$

We will *first carry out our* calculations in the case that

Fig. 2.1 Geometry of the conical horn

$\bar{F} \equiv 0$ and $A \neq 0$. In a spherical coordinate system $\bar{A} = (\bar{A}_r, \bar{A}_\Theta, \bar{A}_\phi)$, where

$$\bar{A}_r = \bar{A}_r \ (r, \Theta, \phi) \ \bar{i}_r \quad ,$$

$$\bar{A}_\Theta = \bar{A}_\phi \ (r, \Theta, \phi) \ \bar{i}_\Theta \quad ,$$

$$\bar{A}_\phi = \bar{A}_\phi \ (r, \Theta, \phi) \ \bar{i}_\phi \quad ,$$

$\bar{i}_r$, $\bar{i}_\Theta$ and $\bar{i}_\phi$ being the unit vectors in a spherical coordinate system. As we are free to choose $\bar{A}$ and as we want the simplest expression possible, we let $\bar{A}$ depend on one coordinate only, hence

$$\bar{A} = A_r \bar{i}_r \qquad \text{and} \qquad \bar{F} \equiv 0 \quad .$$

In a spherical coordinate system (see Appendix B)

$$\nabla \times \bar{A} = \frac{1}{r \sin \Theta} \left[\frac{\partial}{\partial \Theta} (A_\phi \sin \Theta) - \frac{\partial A_\Theta}{\partial \phi} \right] \bar{i}_r + \frac{1}{r} \left[\frac{1}{\sin \Theta} \frac{\partial A_r}{\partial \phi} - \frac{\partial}{\partial r} (rA_\phi) \right] \bar{i}_\Theta$$

$$+ \frac{1}{r} \left[\frac{\partial}{\partial r} (rA_\Theta) - \frac{\partial A_r}{\partial \Theta} \right] \bar{i}_\phi \quad . \tag{B3}$$

As $\bar{A}$ depends only on the coordinate r, Eq.(B3) reduces to

$$\nabla \times (A_r \bar{i}_r) = \frac{1}{r \sin \Theta} \cdot \frac{\partial A_r}{\partial \phi} \bar{i}_\Theta - \frac{1}{r} \frac{\partial A_r}{\partial \Theta} \bar{i}_\phi \quad . \tag{2.17}$$

In accordance with Eq. (2.5) the field vector $\bar{H}$ can now be written in its spherical components:

$$H_r = 0 \tag{2.18}$$

$$H_\Theta = \frac{1}{r \sin \Theta} \frac{\partial A_r}{\partial \phi} \tag{2.19}$$

$$H_\phi = - \frac{1}{r} \frac{\partial A_r}{\partial \Theta} \quad . \tag{2.20}$$

The components in spherical coordinates of the vector $\bar{A}$ can be found from the equations (2.18), (2.19), (2.20), (2.5) and (B3) giving

$$(\nabla \times \nabla \times \bar{A})_r = \frac{1}{r \sin \Theta} \left[\frac{\partial}{\partial \Theta} \left\{ - \frac{\sin \Theta}{r} \cdot \frac{\partial A_r}{\partial \Theta} \right\} - \frac{\partial}{\partial \phi} \left\{ \frac{1}{r \sin \Theta} \frac{\partial A_r}{\partial \phi} \right\} \right] \qquad (2.21)$$

$$(\nabla \times \nabla \times \bar{A})_\Theta = \frac{\partial^2 A_r}{r \, \partial r \partial \Theta} \qquad (2.22)$$

$$(\nabla \times \nabla \times \bar{A})_\phi = \frac{1}{r \sin \Theta} \cdot \frac{\partial^2 A_r}{\partial r \, \partial \phi} \quad . \qquad (2.23)$$

We are now able to solve Eq. (2.9) if the quantity $\nabla \Phi_A$ is also written in its spherical coordinates. For that case we will use equations found in Appendix B:

$$\nabla \Phi_A = \frac{\partial \Phi_A}{\partial r} \bar{i}_r + \frac{1}{r} \frac{\partial \Phi_A}{\partial \Theta} \bar{i}_\Theta + \frac{1}{r \sin \Theta} \frac{\partial \Phi_A}{\partial \phi} \bar{i}_\phi \quad . \qquad B.1)$$

If we substitute the equations (2.21), (2.22), (2.23) and (B.1), the Θ and ϕ components will give rise to the following equations

$$\frac{\partial^2 A_r}{\partial r \, \partial \Theta} = - j \omega \varepsilon \frac{\partial \Phi_A}{\partial \Theta} \qquad (2.24)$$

and

$$\frac{\partial^2 A_r}{\partial r \, \partial \phi} = - j \omega \varepsilon \frac{\partial \Phi_A}{\partial \phi} \quad . \qquad (2.25)$$

The quantity Φ_A is still an arbitrary scalar $\left[\text{Eq. (2.8)} \right]$. If we take

$$- j \omega \varepsilon \Phi_A = \frac{\partial A_r}{\partial r} \quad , \qquad (2.26)$$

the equations (2.24) and (2.25) become identities. If we substitute in Eq. (2.9) the equation $\bar{E} = \frac{1}{j \omega \varepsilon} \nabla \times \bar{H}$ and use for Φ_A the Eq. (2.26), it is readily shown that

$$E_r = \frac{1}{j \omega \varepsilon} \left[\frac{\partial^2 A_r}{\partial r^2} + k^2 A_r \right] \quad . \qquad (2.27)$$

The Θ and ϕ components of the field vector $\bar{A}$ can be derived immediately from the equations (2.22) and (2.23) as $\bar{E} = \frac{1}{j \omega \varepsilon} \nabla \times \nabla \times \bar{A}$, giving

$$E_\Theta = \frac{1}{j \omega \varepsilon r} \frac{\partial^2 A_r}{\partial r \, \partial \Theta} \qquad (2.28)$$

$$E_\phi = \frac{1}{j \omega \varepsilon r \sin \Theta} \frac{\partial^2 A_r}{\partial r \, \partial \phi} \quad . \qquad (2.29)$$

Expanding Eq. (2.9), if we use the r component of Eq. B.1 for the scalar Φ_A (ref.1, p.267) and Eq. (2.21), the r component of Eq. (2.9) becomes

$$\frac{\partial^2 A_r}{\partial r^2} + \frac{1}{r^2 \sin \theta} \frac{\partial}{\partial \theta} \left\{ \sin \theta \frac{\partial A_r}{\partial \theta} \right\} + \frac{1}{r^2 \sin^2 \theta} \frac{\partial^2 A_r}{\partial \phi^2} + k^2 A_r = 0 \qquad (2.30)$$

This equation represents the scalar Helmholtz equation for spherical coordinates and it can be shown that the equation is equivalent to

$$\Delta \psi_A + k^2 \psi_A = 0$$

where $\psi_A = \dfrac{A_r}{r}$ is a solution of the Helmholtz equation. The Helmholtz equation in spherical coordinates in ψ_A, namely

$$\frac{1}{r^2} \frac{\partial}{\partial r} \left\{ r^2 \frac{\partial \psi_A}{\partial r} \right\} + \frac{1}{r^2 \sin \theta} \frac{\partial}{\partial \theta} \left\{ \sin \theta \frac{\partial \psi_A}{\partial \theta} \right\} + \frac{1}{r^2 \sin^2 \theta} \frac{\partial^2 \psi_A}{\partial \phi^2} + k^2 \psi_A = 0$$

$$(2.31)$$

can be solved using the method of separation of variables, if we let

$$\psi_A = R(r) \ H(\theta) \ \Phi(\phi) \ . \qquad (2.32)$$

This method has been described elsewhere (ref.1, p.265) giving the following trio of separated equations:

$$\frac{d}{dr} \left[r^2 \frac{dR}{dr} \right] + \left[(kr)^2 - \nu(\nu + 1) \right] R = 0 \qquad (2.33)$$

$$\frac{1}{\sin \theta} \frac{d}{d\theta} \left[\sin \theta \frac{dH}{d\theta} \right] + \left[\nu(\nu + 1) - \frac{\mu^2}{\sin^2 \theta} \right] H = 0 \qquad (2.34)$$

$$\frac{d^2 \Phi}{d\phi^2} + \mu^2 \Phi = 0 \qquad (2.35)$$

μ and ν being separation constants.

Eq. (2.33) is related to the Bessel equation. The solutions are

called spherical Bessel functions with an arbitrary solution $b_\nu(kr)$ related to cylindrical Bessel functions by

$$b_\nu(kr) = \sqrt{\frac{\pi}{2kr}} \cdot B_{\nu+\frac{1}{2}}(kr) \qquad (App.C)$$

Eq. (2.34) is related to the Legendre equation with the solution

$$L_\nu^\mu \cos \Theta \qquad (App.D)$$

Eq. (2.35) has harmonic solutions like $\cos \mu\phi$, $\sin \mu\phi$, $e^{j\mu\phi}$, $e^{-j\mu\phi}$, etc., or commonly named $h(\mu\phi)$.

If $A_r = r\psi_A$ we have solutions such as

$$A_r = krb_\nu(kr) \cdot L_\nu^\mu \cos \Theta \cdot h(\mu\phi) \qquad (2.36)$$

A possible choice will be (see also Appendices C and D),

$$A_r = kr \, \{C_1 h_\nu^{(1)}(kr) + C_2 h_\nu^{(2)}(kr)\} \, \{C_3 P_\nu^\mu(\cos \Theta) + C_4 Q_\nu^\mu(\cos \Theta)\} \, x$$

$$x \, \{C_5 \cos \mu\phi + C_6 \sin \mu\phi\} \, . \qquad (2.37)$$

The same procedure can be followed if $\bar{A} \equiv 0$ and $\bar{F} = F_r \bar{i}_r$. In accordance with the duality principle we shall find in that case that $E_r = 0$. We may draw here the conclusion that these waves are TE to r. In the same manner the equations (2.18) to (2.20) prove that $\bar{A} = A_r \bar{i}_r$, and $\bar{F} \equiv 0$ gives waves TM to r.

2.5 Field components in spherical coordinates for an arbitrary field

Generally $\bar{A} = A_r \bar{i}_r$ and $\bar{F} = F_r \bar{i}_r$. In the case that both $H_r \neq 0$ and $E_r \neq 0$, we choose A_r so that it satisfies:

$$E_r = \frac{1}{j\omega\varepsilon} \left[\frac{\partial^2 A_r}{\partial r^2} + k^2 A_r \right] \qquad (2.27)$$

In the same way we choose F_r to satisfy the dual equation of Eq. (2.27), viz.

$$H_r = \frac{1}{j\omega\mu} \left[\frac{\partial^2 F_r}{\partial r^2} + k^2 F_r \right] \qquad (2.38)$$

We can now tabulate all the field components which are the sum
of a TM and a TE field expanding Eqs.(2.14) and (2.15) (ref.1,p.269).

$$E_r = \frac{1}{j\omega\epsilon} \left[\frac{\partial^2 A_r}{\partial r^2} + k^2 A_r \right] \qquad (2.39)$$

$$H_r = \frac{1}{j\omega\mu} \left[\frac{\partial^2 F_r}{\partial r^2} + k^2 F_r \right] \qquad (2.40)$$

$$E_\Theta = - \frac{1}{r \sin\Theta} \frac{\partial F_r}{\partial\phi} + \frac{1}{j\omega\mu r} \frac{\partial^2 A_r}{\partial r\, \partial\Theta} \qquad (2.41)$$

$$H_\Theta = \frac{1}{r \sin\Theta} \frac{\partial A_r}{\partial\phi} + \frac{1}{j\omega\epsilon r} \frac{\partial^2 F_r}{\partial r\, \partial\Theta} \qquad (2.42)$$

$$E_\phi = \frac{1}{r} \frac{\partial F_r}{\partial\Theta} + \frac{1}{j\omega\epsilon r \sin\Theta} \frac{\partial^2 A_r}{\partial r\, \partial\phi} \qquad (2.43)$$

$$H_\phi = - \frac{1}{r} \frac{\partial A_r}{\partial\Theta} + \frac{1}{j\omega\mu r \sin\Theta} \frac{\partial^2 F_r}{\partial r\, \partial\phi} . \qquad (2.44)$$

If A_r exists and $F_r \equiv 0$, the field will be TM to r; if $A_r \neq 0$
and F_r exists, the field will be TE to r.

2.6   The field components within an infinite long conical waveguide with circular cross-section

The field equations which have been deduced in the previous sections
can very well be used to calculate the fields within a circular
conical waveguide. For this purpose we will consider the field
components of a wave which is propagated in the direction $\bar{r}$ for
r > 0.

First some modifications to the solution supplied by Eq. (2.37) of
the differential equation (2.9) are introduced.

The harmonic solution h ($\mu\phi$) can only exist if μ is an integer.
The solution is still arbitrary if we choose $\mu=m$ and m $\geq$ 0.

A further simplification might be achieved, if the coordinates
are taken in such a way that h(mϕ) = sin mϕ.

The arbitrary solutions of the Legendre equation L_ν^m (cosΘ) can
be further limited if we notice that L_ν^m (cosΘ) should be finite

for $0 \leq \Theta \leq \pi$. In that case (see App. D)

$$L_\nu^m (\cos \Theta) = P_\nu^m (\cos \Theta),$$

where ν can be found from the boundary conditions.
Finally, as we consider long distances r, where a travelling
wave in direction $\bar{r}$ should be present,

$$b_\nu (kr) = h_\nu^{(2)} (kr) \qquad , \text{ being a Hankel function}$$
of the second kind (App. C).
A possible solution for A_r and F_r will be

$$A_r = C_A \cdot kr \cdot h_\nu^{(2)} (kr) P_\nu^m (\cos \Theta) \sin m\phi \tag{2.45}$$

$$F_r = C_F \cdot kr \cdot h_{\nu'}^{(2)} (kr) P_{\nu'}^m (\cos \Theta) \sin m\phi \text{ ,} \tag{2.46}$$

where ν is found from the boundary conditions for TM_r waves
and ν' from the boundary conditions for TE_r waves.
Using recurrence relations for $b_r (kr)$ (see Appendix C 3.5), we
find that

$$\frac{d}{dx} \left[x b_\nu (x) \right] = b_\nu (x) + x b_\nu' (x) \tag{2.47}$$

$$\frac{d^2}{dx^2} \left[x b_\nu (x) \right] = x b_\nu (x) \left\{ \frac{\nu(\nu + 1)}{x^2} - 1 \right\} \tag{2.48}$$

If Eqs. (2.47) and (2.48) are used in combination with the
Eqs. (2.39) to (2.44), we find the following field components
for TM waves

$$E_r = -jC_A \frac{\nu(\nu + 1)}{\omega \varepsilon r} h_\nu^{(2)} (kr) P_\nu^m (\cos \Theta) \sin m\phi \tag{2.49}$$

$$H_r = 0 \tag{2.50}$$

$$E_\Theta = jC_A \frac{k \sin \Theta}{\omega \varepsilon r} \left[h_\nu^{(2)} (kr) + kr \, h_\nu^{(2)'} (kr) \right] P_\nu^{m'} (\cos \Theta) \sin m\phi \tag{2.51}$$

$$H_\Theta = C_A \frac{mk}{\sin \Theta} h_\nu^{(2)} (kr) P_\nu^m (\cos \Theta) \cos m\phi \tag{2.52}$$

$$E_\phi = -jC_A \frac{mk}{\omega\varepsilon r \sin\Theta}\left[h_\nu^{(2)}(kr) + kr\, h_\nu^{(2)'}(kr)\right] P_\nu^m \cos\Theta \cos m\phi \quad (2.53)$$

$$H_\phi = C_A k \sin\Theta\, h_\nu^{(2)}(kr)\, P_\nu^{m'}(\cos\Theta) \sin m\phi \quad . \qquad (2.54)$$

For TE waves we will find

$$E_r = 0 \qquad (2.55)$$

$$H_r = -jC_F \frac{\nu'(\nu'+1)}{\omega\mu r} h_{\nu'}^{(2)}(kr)\, P_{\nu'}^m(\cos\Theta) \sin m\phi \qquad (2.56)$$

$$E_\Theta = -C_F \frac{mk}{\sin\Theta} h_{\nu'}^{(2)}(kr)\, P_{\nu'}^m(\cos\Theta) \cos m\phi \qquad (2.57)$$

$$H_\Theta = jC_F \frac{k\sin\Theta}{\omega\mu r}\left[h_{\nu'}^{(2)}(kr) + kr\, h_{\nu'}^{(2)'}(kr)\right] P_{\nu'}^{m'}(\cos\Theta) \sin m\phi \qquad (2.58)$$

$$E_\phi = -C_F k \sin\Theta\, h_{\nu'}^{(2)}(kr)\, P_{\nu'}^{m'}(\cos\Theta) \sin m\phi \qquad (2.59)$$

$$H_\phi = -jC_F \frac{mk}{\omega\mu r \sin\Theta}\left[h_{\nu'}^{(2)}(kr) + kr\, h_{\nu'}^{(2)'}(kr)\right] P_{\nu'}^m(\cos\Theta) \cos m\phi \quad . \qquad (2.60)$$

The boundary conditions can be found assuming that the waveguide boundary is a perfect conductor. These conditions require that the tangential component of the electric field vanishes at the boundary. Therefore, there will be no tangential electric field component at the surface of the horn or $E_\phi = 0$, and consequently the boundary condition for TM waves will be

$$P_\nu^m(\cos\Theta)_{\Theta=\alpha} = 0 \qquad (2.61)$$

and for TE waves

$$\left[\frac{d}{d\Theta} P_{\nu'}^m(\cos\Theta)\right]_{\Theta=\alpha} = -\sin\alpha\, P_{\nu'}^{m'}(\cos\alpha) \quad , \qquad (2.62)$$

2.7 Characteristics of conical waveguides

In this section some characteristic quantities of conical waveguides will be discussed, to obtain a clearer insight into the physical behaviour of the fields within a conical waveguide. Partly the work of Barrow and Chu (ref. 2) and Schorr and Beck (ref. 3) will be dealt with in this section as well.

The propagation constant for exponentially propagated waves $\gamma_\nu = \alpha_\nu + \beta_\nu$, where α_ν is the attenuation constant and β_ν the phase constant, may be defined as the logarithmic rate of decrease of magnitude and of change of phase

$$\gamma_\nu = -\frac{1}{u} \frac{\partial u}{\partial r} = -\frac{\partial}{\partial r} \ln u \quad , \tag{2.63}$$

where u represents any component of the field and the wave is propagated in the direction r.

It can be proved (ref. 2) that for increasing r where $r \gg \lambda$, the phase constant β_ν and approaches k.

The phase velocity v_p and the wavelength λ_h of the waves within the horn are given by $v_p = \omega/\beta_\nu$ and $\lambda_h(u,r) = \frac{2\pi}{\beta_\nu}$; the group velocity v_g is given by $v_g = d\omega/d\beta_\nu$.

The characteristic wave impedance in the radial direction is given by

$$Z_\nu(r) = \frac{E_\Theta}{H_\phi} = -\frac{E_\phi}{H_\Theta} \quad . \tag{2.64}$$

From the Eqs. (2.49) to (2.60) it is readily seen that Z_ν is independent of Θ and ϕ but it is a function of the cone angle α and the mode ν.

It is common practice (ref. 4) to distinguish 3 regions in which $\gamma_\nu(u,r)$ and $Z_\nu(r)$ have a different behaviour.

In the region $kr \ll \nu + \frac{1}{2}$ the phase constant $\beta \ll \frac{2\pi}{\lambda}$ but it increases rapidly with r until it approaches the value $\frac{2\pi}{\lambda}$ which is the phase constant in free space. The group velocity is very low, almost zero. Therefore the signal will be propagated at a low velocity. The waves have apparently a hybrid character, being a mixture of standing and travelling waves (ref. 2).

This region is often called the attenuation region.
The wave impedance is mainly inductive for TE waves and
capacitive for TM waves. If r is increased, the real part
of Z_ν increases as well, while the imaginary part decreases.
It has been found by Schorr and Beck (ref. 3) that the wave
impedance in the attenuation region can be approximated by

$$Z_{\nu,E} \approx \sqrt{\frac{\mu}{\epsilon}} \left[\frac{\pi \cdot (2\nu + 1)}{\nu \, \Gamma(\nu + \frac{1}{2}) \cdot \Gamma(\nu + \frac{3}{2})} \cdot \left(\frac{kr}{2}\right)^{2\nu+2} + j\frac{4}{\nu kr} \right] \qquad (2.65)$$

$$Z_{\nu,M} \approx \sqrt{\frac{\mu}{\epsilon}} \left[\frac{\pi \cdot (2\nu + 1)}{\Gamma(\nu + \frac{1}{2}) \cdot \Gamma(\nu + \frac{3}{2})} \cdot \left(\frac{kr}{2}\right)^{2\nu} - \frac{j\nu}{kr} \right] \qquad (2.66)$$

Γ being the gamma function as explained elsewhere (ref. 5, 6.1.6).

Within the region $kr \approx \nu+\frac{1}{2}$ the impedance becomes more real.
Bucholtz (ref. 4) has calculated for TE waves and $kr = \nu+\frac{1}{2}$

$$Z_{\nu,E} \approx \sqrt{\frac{\mu}{\epsilon}} \cdot 2 \left[\frac{\Gamma(\frac{2}{3})}{\Gamma(\frac{1}{3})} \cdot \left(\frac{6}{\nu+\frac{1}{2}}\right)^{\frac{1}{3}} (j - \sqrt{3}) - \frac{j}{\nu+\frac{1}{2}} \right]^{-1} \quad ,$$

where

$$\frac{\Gamma(\frac{2}{3})}{\Gamma(\frac{1}{3})} \approx \frac{1.35}{2.68} \approx 0.5 \qquad . \qquad (2.67)$$

For our purpose the transmission region $kr \gg \nu+\frac{1}{2}$ is most important.
The behaviour of the waves in this region approaches asymtotically
to that of travelling waves in free space.
If r decreases, and consequently the radius of the horn increases,
the influence of the walls of the cone becomes smaller.
For both TM and TE waves the wave impedance approaches to $\sqrt{\frac{\mu}{\epsilon}}$ (ref.4) and
the propagation constant

$$\gamma = \alpha + j\beta = \frac{1}{r} + jk$$

if the field is expressed as $u = \frac{1}{r} e^{-jkr}$.

For a finite horn with a length r_h for which $kr_h \gg \nu+\frac{1}{2}$ the fields
near the aperture do not differ much from the fields at the aperture

of an infinitely long horn. The horn has a wave impedance
which is nearly equal to that of free space and is said to
be well matched to free space.

The quantities mentioned above have only significance if
the field varies harmonically with increasing r; this means
that the opening angle should not be too large (< $40^{\circ}...50^{\circ}$).
If the wall of the conical waveguide has a finite conductivity,
the effect of this is greater in the attenuation region than
in the transmission region. This is explained by Barrow and Chu
(ref. 2), who indicate that the power dissipated in the walls
of the horn is approximately proportional to the square of the
tangential magnetic field strength at the wall. For the same
amount of transmitted power, this magnetic field is much larger
in the attenuation region than in the transmission region, and
so power loss is also greater.

Consequently, the curves of the attenuation constant α as a
function of radial distance will be steeper for practical horns
than for ideal horns with a perfect conductivity (ref. 2, p.56).
We will now determine the above characteristics by using the
equations (2.49) to (2.60) for the wave impedance for TE and TM
waves. We find

$$Z_{\nu,E} = -j \sqrt{\frac{\mu}{\epsilon}} \left[\frac{1}{kr} + \frac{h_{\nu}^{(2)'}(kr)}{h_{\nu}^{(2)}(kr)} \right]^{-1} \tag{2.68}$$

and

$$Z_{\nu,M} = j \sqrt{\frac{\mu}{\epsilon}} \left[\frac{1}{kr} + \frac{h_{\nu}^{(2)'}(kr)}{h_{\nu}^{(2)}(kr)} \right] . \tag{2.69}$$

It is readily seen that

$$Z_{\nu,E} \cdot Z_{\nu,M} = \frac{\mu}{\epsilon} . \tag{2.70}$$

These expressions for the wave impedance depend on ν but can be
used for any different flare angle.

From Eqs. (2.49) to (2.60) expressions are also to be found for
the propagation constant γ.

Eqs. (2.49), (2.52) and (2.54) for TM waves and (2.56), (2.57) and (2.59) for TE waves will lead to the propagation constant

$$\gamma_{1,\nu} = -k \frac{h_\nu^{(2)'}(kr)}{h_\nu^{(2)}(kr)} \tag{2.71}$$

while Eqs. (2.51) and (2.53) for TM waves and Eqs. (2.58) and (2.60) for TE waves result in a different propagation constant

$$\gamma_{2,\nu} = -k \left[\frac{1}{x} \left\{ h_\nu^{(2)}(x) + x h_\nu^{(2)'}(x) \right\} \right]^{-1} \cdot \frac{\partial}{\partial x} \left[\frac{1}{x} \left(h_\nu^{(2)}(x) + x h_\nu^{(2)'}(x) \right) \right]_{x=kr} \tag{2.72}$$

In all cases Eq. (2.63) has been used.

Eq. (2.72) can be simplified by realising that (see also App. C 47)

$$\frac{\partial}{\partial x} \left[\frac{1}{x} (b_\nu(x) + x b_\nu'(x)) \right] = -\frac{1}{x^2} (b_\nu(x) + x b_\nu'(x) + \frac{1}{x} \frac{\partial^2}{\partial x^2} (x b_\nu(x))$$

$$= -\frac{1}{x^2} (b_\nu(x) + x b_\nu'(x)) + b_\nu(x) \left(\frac{\nu(\nu+1)}{x^2} - 1 \right) . \tag{2.73}$$

Therefore,

$$\gamma_{2,\nu} = -k \left[-\frac{1}{x} + \frac{x h_\nu^{(2)}(x) \left(\frac{\nu(\nu+1)}{x^2} - 1 \right)}{h_\nu^{(2)}(x) + x h_\nu^{(2)'}(x)} \right]_{x=kr} \quad \text{or}$$

$$\gamma_{2,\nu} = k \left[\frac{1}{x} + \frac{1 - \frac{\nu(\nu+1)}{x^2}}{\frac{1}{x} + \frac{h_\nu^{(2)'}(x)}{h_\nu^{(2)}(x)}} \right]_{x=kr} . \tag{2.74}$$

As will be noticed from Eqs. (2.68), (2.69) and (2.74), the behaviour of Z_ν and γ_ν is mainly determined by the factor

$$\frac{1}{x} + \frac{h_\nu^{(2)'}(x)}{h_\nu^{(2)}(x)} \Bigg|_{x=kr} .$$

This factor can be simplified in accordance with the method followed in Appendix C (Sec. 3.6) to

$$\frac{1}{2x} + \frac{H_{\nu+\frac{1}{2}}^{(2)}(x)}{H_{\nu+\frac{1}{2}}(x)} \Bigg|_{x=kr}$$

which approaches for $x \gg 1$ and $x \gg \nu$ to $-j$. (Appendix C3.6).
Therefore Z_ν and γ_ν will approach their free space values
if the following conditions are fulfilled:

$$(kr)^2 \gg \nu^2 \qquad \text{for} \qquad \gamma_{2,\nu}$$

$$kr \gg \nu \qquad \text{for} \qquad Z_{\nu,E} , \ Z_{\nu,M} \text{ and } \gamma_{1,\nu}$$

$$\text{and} \quad kr \gg 1 \qquad \text{for} \quad \gamma_{1,\nu}, \ \gamma_{2,\nu}, \ Z_{\nu,E} \text{ and } Z_{\nu,M} . \qquad (2.75)$$

Bucholtz (ref. 4) derives complicated expressions for $Z_{\nu,E}$ in
the attenuation region, the transmission region and also in
the region $kr \approx \nu+\frac{1}{2}$.
The equations are not mentioned here as they are not used any
further. Interesting, however, is the dependence of the real and
imaginary part of $Z_{\nu,E}$ as a function of ν.
Once values have been found for $Z_{\nu,E}$, it is not difficult to
find values for $Z_{\nu,M}$ using Eq. (2.70).
It will be proved in this chapter that the conical horn is well
matched to free space if $kr \gg \nu$ for the highest mode we want
to use.
The mismatch is readily found by using the expression of Bucholtz
for $Z_{\nu,E}$ if $kr \to \infty$:

$$Z_{\nu,E} \sim 120 \ \pi \left[1 + \frac{(2\nu + 1)^2 - 1}{8(kr)^2} \ (1 + \frac{j}{kr}) + \ldots \right]$$

$$\sim 120 \ \pi \left[1 + \frac{(2\nu + 1)^2}{8(kr)^2} \right] , \ \nu \text{ and } kr \text{ being large} \qquad (2.76)$$

If the mismatch should not increase by 1% it is readily seen that
the minimum length of the horn should be at least

$$r_{min} \geq (\nu + \frac{1}{2})\lambda . \qquad (2.77)$$

The requirements with regard to the matching of the horn to free
space are not the only factors to be considered when dimensioning
a horn.
Very important is also the required beamwidth, which is in close
relationship with the aperture (ref. 6, p.193).
Mostly no problem arises if small beamwidths are required, but
if the aperture should be smaller than is advisable for correct
matching, attention should be paid to the method of Geyer (ref.7).
He surrounded the horn edge by one or more conducting collars
which act as short-circuit quarter wavelength stubs. It appears
that in this case the mismatch of the horn decreases considerably.

2.8 The fields in the transmission region

In this section the fields in the transmission region are
calculated for the case that the flare angle is small and
the distance from the fieldpoint to the apex is large. This
is done to enable the field in the aperture of a conical
horn to be compared with a conical waveguide.
We will give only relations for TE waves.
If TM waves are required they may be readily found by means
of the duality principles.
We will consider the equations (2.55) to (2.60) and introduce
some modifications. If the flare angle α of the cone is small
and the distance r from the fieldpoint to the apex is large we
can write, in accordance with Appendix D.5,

$$P_\nu^m (\cos \Theta) = \left[-\psi'\right]^m J_m (\psi) \left[1 + 0(\sin \tfrac{\Theta}{2})^2\right] \qquad (2.78)$$

and

$$\frac{d}{d\Theta} P_\nu^m (\cos \Theta) \approx - \sin \Theta \; P_\nu^{m'} (\cos \Theta) =$$

$$- \left[\psi'\right]^{m+1} J_m' (\psi) \left[1 + 0(\sin \tfrac{\Theta}{2})^2\right] , \qquad (2.79)$$

where

$$\psi = (2\nu + 1) \sin \tfrac{1}{2} \Theta \qquad (2.80)$$

and

$$\psi' = \frac{d\psi}{d\Theta} = (\nu + \tfrac{1}{2}) \cos \tfrac{1}{2} \Theta \quad . \qquad (2.81)$$

Further,

$$\sin^2 \tfrac{1}{2}\Theta = \tfrac{1}{2} \left[1 - \cos\Theta\right] = \tfrac{1}{2} \left[1 - 1 + \tfrac{1}{2}\Theta^2 - \tfrac{1}{24} \Theta^4 + \ldots\right]$$

$$= (\tfrac{1}{2}\Theta)^2 \left[1 - 0(\tfrac{\Theta^2}{12})\right] \quad . \qquad (2.82)$$

Even for $\Theta = 20^O$ the error in Eqs. (2.78) and (2.79) is not more than 3% (See also Appendix D.3). Substitution of the results obtained here in the Eqs. (2.55) to (2.60) yields in the following field equations for the TE waves:

$$E_r = 0$$

$$H_r = -jC_F \frac{\nu'(\nu'+1)}{\omega\mu r} h_{\nu'}^{(2)} (kr) \left[-(\nu'+\tfrac{1}{2}) \cos \tfrac{1}{2}\Theta\right]^m \, J_m \left\{(2\nu'+1) \sin \tfrac{1}{2}\Theta\right\} \sin m\phi$$

(2.83)

$$E_\Theta = -C_F \frac{mk}{\sin \Theta} h_{\nu'}^{(2)}(kr) \left[-(\nu'+\tfrac{1}{2}) \cos \tfrac{1}{2}\Theta\right]^m \, J_m \left\{(2\nu'+1) \sin \tfrac{1}{2}\Theta\right\} \cos m\phi$$

(2.84)

$$E_\phi = -C_F \, k \, h_{\nu'}^{(2)}(kr) \left[-(\nu'+\tfrac{1}{2}) \cos \tfrac{1}{2}\Theta\right]^{m+1} \, J_m' \left\{(2\nu'+1) \sin \tfrac{1}{2}\Theta\right\} \sin m\phi$$

(2.85)

$$H_\Theta = - \frac{E_\phi}{Z_{\nu',E}}$$

(2.86)

$$H_\phi = \frac{E_\Theta}{Z_{\nu',E}}$$

(2.87)

From Appendix C it is explained that

$$h_\nu^{(2)} (kr) = \frac{1}{x} \left[j e^{-j(x- \frac{\nu}{2}\pi)} + 0 \left(\frac{1-j}{x\sqrt{x}}\right)\right]_{x=kr}$$

(App.C.35)

If we use this relation, Eqs. (2.84) and (2.85) may be written as

$$E_\Theta = C_{M,1} \, J_m \left[(2\nu'+1) \sin \tfrac{1}{2}\Theta\right] \cos m\phi \, e^{-jkr}$$

(2.88)

and

$$E_\phi = C_{M,2} \, J_m' \left[(2\nu'+1) \sin \tfrac{1}{2}\Theta\right] \sin m\phi \, e^{-jkr}$$

(2.89)

where, assuming that α is small and kr large,

$$C_{M,2} = -jC_F \frac{1}{r} \exp\left[j \frac{v'}{2} \pi\right]\left[-(v'+\tfrac{1}{2}) \cos \tfrac{1}{2}\Theta\right]^{m+1} \qquad (2.90)$$

and

$$C_{M,1} = -C_{M,2} \frac{m}{\sin \Theta} \frac{1}{(v'+\tfrac{1}{2}) \cos \tfrac{1}{2}\Theta} = -C_{M,2} \frac{1}{(\cos \tfrac{1}{2}\Theta)^2} \frac{m}{(2v'+1) \sin \tfrac{1}{2}\Theta}$$

$$= -C_{M,2} \frac{1}{(\cos \tfrac{1}{2}\Theta)^2} \frac{m}{\kappa' r \Theta} \qquad . \qquad (2.91)$$

In Eq. (2.91) κ' is by definition

$$\kappa' = \frac{1}{r\Theta} (2v'+1) \sin \tfrac{1}{2}\Theta \qquad (2.92)$$

which for small Θ turns into

$$\kappa' = \frac{v'+\tfrac{1}{2}}{r} \qquad . \qquad (2.93)$$

It is also possible to determine values for v and v' from the boundary conditions.

From Eqs. (2.61) and (2.78) we find for TM waves

$$P_v^m (\cos \alpha) = \left[-(v+\tfrac{1}{2}) \cos \tfrac{1}{2}\alpha\right]^m . J_m\left\{(2v+1) \sin \tfrac{1}{2}\alpha\right\} = 0$$

or

$$J_m\left\{(2v+1) \sin \tfrac{1}{2}\alpha\right\} = 0 \ , \ \text{as} \ \alpha < \frac{\pi}{2}$$

If we call $(2v+1) \sin \tfrac{1}{2}\alpha = \varepsilon_{mn}$, ε_{mn} will represent the nth zero point of the function $J_m(x)$. For every value of ε_{mn} there will be a value of v. Therefore we obtain as boundary value for the $TM_{mn,r}$ mode

$$v_{mn} = \tfrac{1}{2}\left[\frac{\varepsilon_{mn}}{\sin \tfrac{1}{2}\alpha} - 1\right] \qquad . \qquad (2.94)$$

If the flare angle α is small, ν_{mn} will be large. In the same way boundary conditions for TE waves are found using the Eqs. (2.62) and (2.79) or

$$J_m' (\psi) = 0$$

resulting in

$$\nu_{mn}' = \tfrac{1}{2} \left[\frac{\epsilon_{mn}'}{\sin \tfrac{1}{2}\alpha} - 1 \right] \quad , \tag{2.95}$$

where ϵ_{mn}' is the nth zero point of $J_m'(x)$.

2.9 Comparison of circular waveguides and conical horns

The field expressions for waves in circular waveguides are found in several textbooks (ref. 6) and will therefore not be deduced here in detail. If the cylinder coordinates ρ, ϕ and z are used (Fig. 2.2) and we calculate the fields in an infinite circular waveguide, we find expressions which are very similar to those found for infinite conical waveguides.
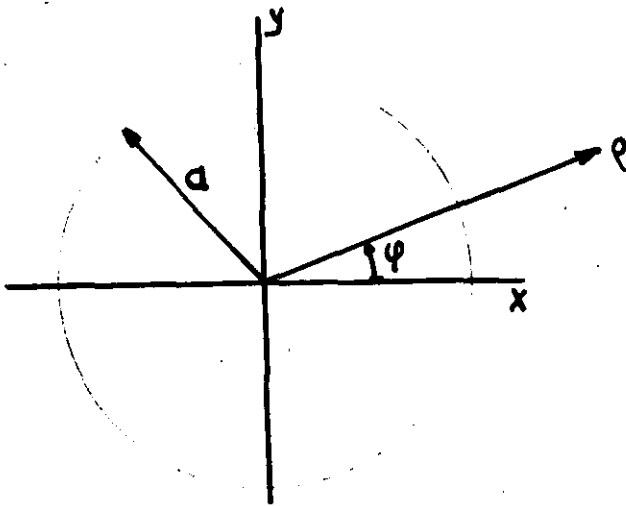
For reasons of simplicity we discuss here only the circular waveguide components E_ρ and E_φ for TE waves. The other field components of TE waves and the components of the TM waves give similar results.

It is found elsewhere (refs. 6, 8) for TE waves polarised in the y direction (Fig. 2.2) that

Fig. 2.2

$$E_\rho = j\omega\mu \cdot \sin m\phi \frac{m J_m(\kappa'\rho)}{\rho} \cdot e^{-\gamma_{mn}z} \tag{2.96}$$

$$E_\phi = j\omega\mu \; \kappa' \; \cos m\phi \; J_m'(\kappa'\rho) \; e^{-\gamma_{mn}z} \quad , \tag{2.97}$$

where $J_m^{'} (\kappa' \rho)_{\rho=a} = 0$, a being the radius of the waveguide.

If the aperture diameter 2a is large compared with the wave-
length, $\gamma_{mn} \approx jk$ (ref. 6, p.205).
If we compare E_ρ with E_Θ from Eq. (2.88), and E_ϕ from Eq. (2.97)
with E_ϕ from Eq. (2.89), we find a great amount of similarity.
If the flare angle of the conical waveguide is small, it is
even possible to convert the field equations for conical waveguides
into those for circular waveguides. In that case the spherical
coordinates have to be converted
into cylindrical coordinates
according to table 3. In this
conversion the original plane
wavefront of the cylindrical
waveguide changes into a
spherical wavefront. Therefore,
ρ corresponds with $r\Theta$ and not
with $r \sin \Theta$, although for small
angles both are nearly equal.
To make complete conversion
possible, there are two
conditions to be met. First of
all the phase constant β should

Table 3

cylindrical coordinates	spherical coordinates
z	r
ρ	$r\Theta$
ϕ	ϕ
U_z	U_r
U_ρ	U_Θ
U_ϕ	U_ϕ

be nearly equal to k, which can be realised if the diameter of the
horn is large ($2a \gg \lambda$), and secondly the flare angle of the cone α
should be so small that for all angles $\Theta, (\cos \tfrac{1}{2}\Theta)^2 \approx 1$, with $\Theta_{max}=\alpha$.
Except for the harmonic terms $\sin m\varphi$ and $\cos m\varphi$ the equations
for conical waveguides and circular waveguides are now similar
and interchangeable using table 4.

Table 4

circular waveguide	conical waveguide
e^{-jkz}	e^{-jkr}
κ'	$\dfrac{1}{r\Theta} (2\nu'+1) \sin \tfrac{1}{2}\Theta \approx (\nu'+\tfrac{1}{2})/r$
$j\omega\mu\kappa'$	$C_{M,2}= -jC_F \dfrac{1}{r} \exp(j\dfrac{\nu'}{2} \pi) \{-(\nu'+\tfrac{1}{2}) \cos \tfrac{1}{2}\Theta\}^{m+1}$

2.10 Conclusion and final remarks

It has been proved in the previous sections that if the dimensions
of a conical horn meet certain requirements, it is possible to
prescribe the aperture fields of a conical horn by means of the
modes of a circular waveguide, however, with a spherical wavefront.
The requirements which the horn has to meet can be given only
roughly.

(1) The flare angle should be small, i.e.

$$(\cos \tfrac{1}{2}\alpha)^2 \approx 1$$

although according to Appendix D (Sec. 3) this requirement
is not very severe.

(2) The length of the horn should meet two requirements, viz.

$$\sqrt{kr_h} \gg 1 \qquad \text{and}$$

$$kr_h \gg \nu'$$

which means that the diameter of the horn (2a) should be large
compared with $\tfrac{1}{2}\lambda$.

It is advised to calculate the error for various values of α and ν_h,
preferably by means of a computer.
The phase centre of conical horns with a small flare angle fed by
a circular waveguide is not situated in the cone's apex. If α is
made smaller, the phase centre will move toward the aperture.
If $\alpha = 0$, in the case of circular waveguides the phase centre is
situated in the aperture. If the horn is very short and the aperture
diameter small, it even appears that the phase centre is located in
front of the aperture outside the horn (ref. 18). At the junction
of the circular waveguide and the cone higher modes are excited
but rapidly attenuated. Schorr and Beck (ref. 3) have even calculated
the length of the journey of higher modes in the attenuation region.

3. The near field of a conical horn antenna

3.1 Introduction

The conical horn antenna is often used as a primary radiator for
near field cassegrain antenna systems. Although the far field
is treated very well in several handbooks (ref. 6), the near
field is still a subject of discussion. It is often calculated
by means of the integral

$$\bar{E}_p = \frac{jk}{4\pi} \iint\limits_{S} \bar{E}_A \, (1 + \bar{n}.\bar{i}_r) \, \frac{e^{-jkr}}{r} \, dS \qquad (3.1)$$

and the geometry of Fig. 3.1. The integral has been used by
several investigators (refs. 13, 14, 15).
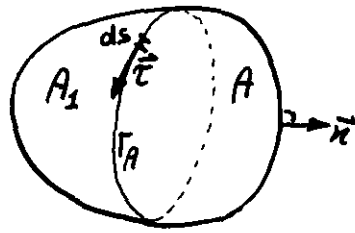
Fig. 3.1

The assumptions which are generally made to justify the use of
Eq. (3.1) are rather vague. It is thought that the assumptions are
justified if the total flare angle of the horn is not too large
and the length of the horn is not too short in terms of wavelength.
In this case the field at the aperture of the horn is the same as
that which exists at the same cross-section of an infinite horn,
neglecting spillover around the rim of the horn. The field is said
to exist at a distance that is at least a few wavelengths from
the mouth of the horn.

The aperture field $\bar{E}_A$ has been taken in accordance with the E_ρ and
E_ϕ components of the TE_{11} mode of a circular waveguide but with a
spherical phase front (see also Eqs. (2.96), (2.97)).

A further assumption without explanation lies in the fact that the
factor $(\bar{E}_A.\bar{i}_r)(\bar{n}+\bar{i}_r)$ in Eq. (3.12) can be neglected with respect to
$\bar{E}_A (1 + \bar{n}.\bar{i}_r)$.

It appears that Eq. (3.1) gives results which very well agree
with measured values. The assumption that the phase centre is
situated at the apex of the cone of the horn is not true in
all cases; it appears that if the flare angle becomes very small,
the phase centre moves towards the aperture. In the case that
the flare angle is zero, the phase centre is situated in the
aperture plane (ref. 6, p. 343).
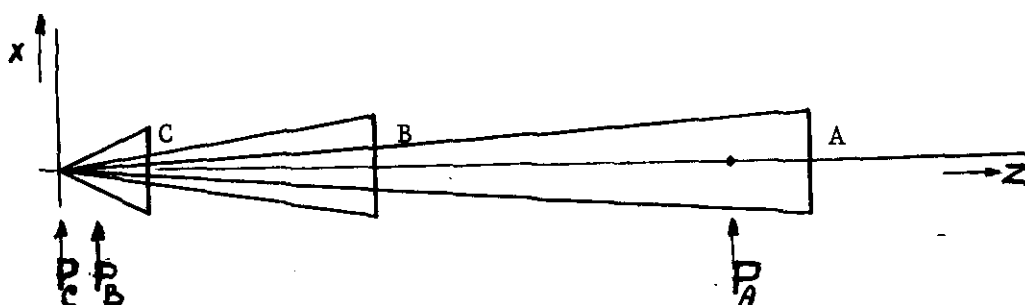Various examples of horns with different flare angles and
their phase centres are shown in Fig. 3.2.

Fig. 3.2

Aperture diameter: $D_A = 12.2\lambda$; $D_B = 14\lambda$; $D_C = 11.3\lambda$

$\frac{1}{2}$ flare angle (α): $\alpha_A = 3.5^{\circ}$; $\alpha_B = 9.5^{\circ}$; $\alpha_C = 25^{\circ}$

length of horn : $b_A = 100\lambda$; $b_B = 53\lambda$; $b_C = 13.4\lambda$

phase centre : $P_A = 89\lambda$; $P_B = 5\lambda$; $P_C \approx 0$

A = ref. 15   B = ref. 14   C = ref. 13

It will be shown in the following sections that Eq. (3.1) can only
be used if the phase centre coincides with the origin of the
coordinate system. Therefore, for horns with a small flare angle
the phase centre will have to be determined before using Eq. (3.1).

3.2 General considerations on the approximations

In discussing the electromagnetic field from a conical horn antenna
we shall make use of the theory of Silver (ref. 6, p.158-160) who
has found that, if the scattered field over a surface is known,
the field at an external point P is given by

$$E_p = \frac{1}{4\pi j\omega\varepsilon} \iint\limits_A \left[k^2(\bar{n} \times \bar{H}_A) \, \psi + \{(\bar{n} \times \bar{H}_A) \cdot \nabla(\nabla\psi) + j\omega\varepsilon(\bar{n} \times \bar{E}_A) \times \nabla\psi \right] dS. \quad (3.2)$$

In this integral $\bar{E}_A$ and $\bar{H}_A$ represent the scattered field over the aperture of the horn according to the geometry of Fig. 3.3.
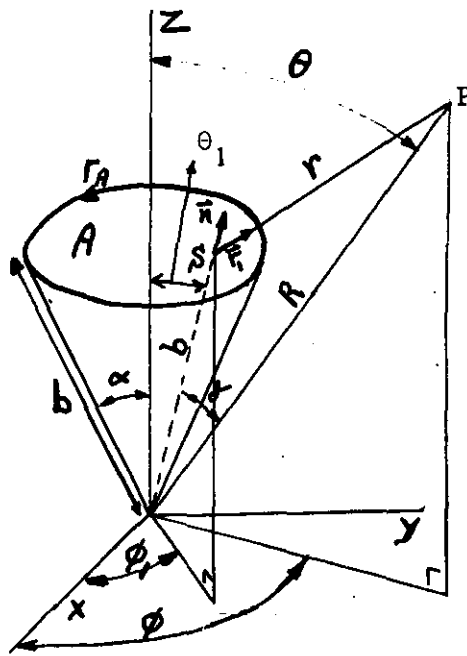
$P(R,\theta,\phi)$: fieldpoint

$S(R_1,\theta_1,\phi_1) = S(b,\theta_1,\phi_1)$: source point

A: spherical surface

Γ_A: circular

phase centre in origin

Fig. 3.3

The conical horn in a spherical coordinate system.

The integral is based on field and charge distributions over a closed surface and a boundary curve Γ_A.

Using the equations B4, B5 and B6 from Appendix B, Eq. (3.2) can be written in a different way. For this purpose we let $\bar{n} \times \bar{H}_A = \bar{U}$ and $\bar{n} \times \bar{E}_A = \bar{V}$, and after some calculation we find

$$E_p = \frac{1}{4\pi j\omega\varepsilon} \iint\limits_A \left[j\omega\varepsilon \cdot jk(1 + \frac{1}{jkr}) \, \bar{V} \times \bar{i}_r - k^2 \, \bar{i}_r \times (\bar{i}_r \times \bar{U}) \right.$$
$$\left. - \frac{jk}{r} \cdot (1 + \frac{1}{jkr}) \, \{\bar{U} - 3(\bar{U} \cdot \bar{i}_r) \, \bar{i}_r\} \right] \psi \, dS \quad (3.3)$$

or

$$E_p = -\frac{jk}{4\pi} \iint\limits_A \left[(1 + \frac{1}{jkr}) \, \bar{i}_r \times \bar{V} - (\frac{\mu}{\varepsilon})^{\frac{1}{2}} \cdot \bar{i}_r \times (\bar{i}_r \times \bar{U}) + \right.$$
$$\left. + (\frac{\mu}{\varepsilon})^{\frac{1}{2}} \frac{1}{jkr} (1 + \frac{1}{jkr}) \, \{\bar{U} - 3(\bar{U} \cdot \bar{i}_r) \, \bar{i}_r\} \right] \psi \, dS \quad (3.4)$$

If we make the assumption that $1 + \frac{1}{jkr} \approx 1$ and use a vector rule for the second term we find

$$E_p = -\frac{jk}{4\pi} \iint\limits_A \left[\bar{i}_r \times \bar{V} - (\tfrac{\mu}{\varepsilon})^{\frac{1}{2}} (\bar{i}_r . \bar{U}) . \bar{i}_r + (\tfrac{\mu}{\varepsilon})^{\frac{1}{2}} \bar{U} + \right.$$

$$\left. + (\tfrac{\mu}{\varepsilon})^{\frac{1}{2}} \frac{1}{jkr} \{ \bar{U} - 3(\bar{U} . \bar{i}_r) \bar{i}_r \} \right] \psi \, dS \qquad (3.5)$$

or

$$E_p = -\frac{jk}{4\pi} \iint\limits_A \left[\bar{i}_r \times \bar{V} + (\tfrac{\mu}{\varepsilon})^{\frac{1}{2}} \bar{U}(1 + \frac{1}{jkr}) - (\tfrac{\mu}{\varepsilon})^{\frac{1}{2}} (\bar{i}_r . \bar{U}) \bar{i}_r (1 + \frac{1}{jkr}) . \right.$$

$$\left. . \{ \frac{1}{1 + jkr} (1 + \frac{3}{jkr}) \} \right]. \qquad (3.6)$$

Approximating once more $1 + \frac{1}{jkr}$ by 1, we finally find

$$E_p = -\frac{jk}{4\pi} \iint\limits_A \left[\bar{i}_r \times \bar{V} - (\tfrac{\mu}{\varepsilon})^{\frac{1}{2}} \bar{i}_r \times (\bar{i}_r \times \bar{U}) \right] \psi \, dS \qquad (3.7)$$

or

$$E_p = -\frac{jk}{4\pi} \iint\limits_A \left[\bar{i}_r \times \{ \bar{n} \times E_A - (\tfrac{\mu}{\varepsilon})^{\frac{1}{2}} \bar{i}_r \times (\bar{n} \times \bar{H}_A) \} \right] \frac{e^{-jkr}}{r} \, dS \qquad (3.8)$$

Eq. (3.8) is subject to the following restrictions.

1. The aperture field is known and spherical and is regarded as primary source.

2. The currents and fields outside the horn are ignored; this is better met if the aperture becomes larger in terms of λ.

3. The integration is carried out over an open surface. To fulfil Maxwell's laws a charge distribution is introduced along the geometrical optical boundary of the aperture. In our case the boundary is in the rim of the horn.

4. $\qquad 1 + \frac{1}{jkr} \approx 1.$

5. The configuration of the horn behind the aperture ($z < b \cos \alpha$, Fig. 3.3) is not taken into consideration.

In accordance with these restrictions Θ may not be too large. If Θ is equal to α or smaller, we may expect good results with Eq. (3.8).
The error made by taking $1 + \frac{1}{jkr} \approx 1$ decreases rapidly.

If, for example, $r = 5\lambda$

$$\left| 1 + \frac{1}{jkr} \right| \approx 1 + 0, 5.10^{-3} \qquad \text{and}$$

$$\text{arc} \left| 1 + \frac{1}{jkr} \right| \approx -2^{\circ}$$

3.3 Approximations for well-matched horns

If the characteristic wave impedance of the horn is equal or nearly equal to that of free space in the aperture (120π ohms), then

$$H = \left(\frac{\varepsilon}{\mu}\right)^{\frac{1}{2}} . \, \bar{s} \times \bar{E} \quad , \tag{3.9}$$

where $\bar{s}$ is a unit vector of the Poynting vector $\bar{S}$. If the origin of the coordinate system corresponds with the phase centre, $\bar{s} = \bar{n}$, therefore,

$$\bar{n}.\bar{H} \equiv \bar{n}.\bar{E} \equiv 0 \tag{3.10}$$

in the spherical aperture plane of the horn (Fig. 3.3). The components from Eq. (3.8) can now be simplified since

$$\bar{i}_r \times (\bar{n} \times \bar{E}_A) = (\bar{i}_r \cdot \bar{E}_A) \, \bar{n} - (\bar{n} \cdot \bar{i}_r) \, \bar{E}_A \quad ,$$

$$\bar{n} \times \bar{H}_A = n \times \left[\sqrt{\frac{\varepsilon}{\mu}} \, \bar{n} \times \bar{E}_A \right] = \left(\frac{\varepsilon}{\mu}\right)^{\frac{1}{2}} \left[(\bar{n} \cdot \bar{E}_A) \, \bar{n} - \bar{E}_A \right] = -\sqrt{\frac{\varepsilon}{\mu}} \, \bar{E}_A ,$$

and

$$-\left(\frac{\mu}{\varepsilon}\right)^{\frac{1}{2}} . \, \bar{i}_r \times \left[\bar{i}_r \times \{-\left(\frac{\varepsilon}{\mu}\right)^{\frac{1}{2}} \bar{E}_A \} \right] = (\bar{i}_r \cdot \bar{E}_A) \cdot \bar{i}_r - \bar{E}_A \; . \tag{3.11}$$

Substituting the expressions (3.11) in Eq. (3.8) this becomes

$$E_p = \frac{jk}{4\pi} \iint_A \left[\bar{E}_A (1 + \bar{n} \cdot \bar{i}_r) - (\bar{E}_A \cdot \bar{i}_r) (\bar{n} + \bar{i}_r) \right] \frac{e^{-jkr}}{r} . \, dS \; , \tag{3.12}$$

which is used by several investigators (refs. 14, 15). If a conical horn is used, the aperture field is assumed to be spherical. In that case the integral can be solved by substituting in Eq. (3.12) the following relations:

$$S = \int_0^{2\pi} \int_0^{\alpha} b^2 \sin \Theta_1 \, d\Theta_1 \, d\phi_1$$

$$r = (b^2 + R^2 - 2bR \cos \gamma)^{\frac{1}{2}}$$

$$\cos \gamma = \bar{n}.\bar{R}_1 = \sin \Theta . \sin \Theta_1 \cos (\phi - \phi_1) + \cos \Theta \cos \Theta_1$$

$$\bar{n}.\bar{i}_r = \frac{R \cos \gamma - b}{r} \quad \text{(see also Fig. 3.3)} \tag{3.13}$$

For most practical cases the contribution of $(\bar{E}_A . \bar{i}_r) (\bar{n} + \bar{i}_r)$ from Eq. (3.12) can be neglected with regard to the contribution of $\bar{E}_A (1 + \bar{n}.\bar{i}_r)$. This seems rather unlikely for cases where the distance from the fieldpoint P to the aperture is smaller than the aperture diameter D. The situation is illustrated in Fig. 3.4.
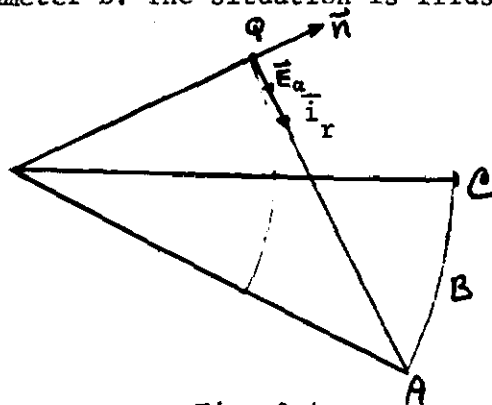
Fig. 3.4

The orientation of $\bar{E}_A$, $\bar{i}_r$ and $\bar{n}$ with respect to fieldpoint A

The contributions of the two terms under discussion to the field in the points A, B and C from the aperture point Q are of the same order. However, as will be explained in the following section, the phase of the factor $\frac{e^{-jkr}}{r}$ in Eq. (3.12) has to be allowed for in the case of field points close to the aperture.

3.4   The theory of Fresnel zones

According to Huygens every point of a wave front may be considered as a centre of a secondary disturbance giving rise to spherical wavelets. The wavefront may be regarded as the equiphase envelope of these wavelets. Fresnel suggested that the secondary wavelets

mutually interfere. The combination of the two theories is what
is known as the Huygens Fresnel principle.

This geometrical optical method gives satisfactory results for
finite wavelengths provided the fieldpoint P (Fig. 3.5) meets
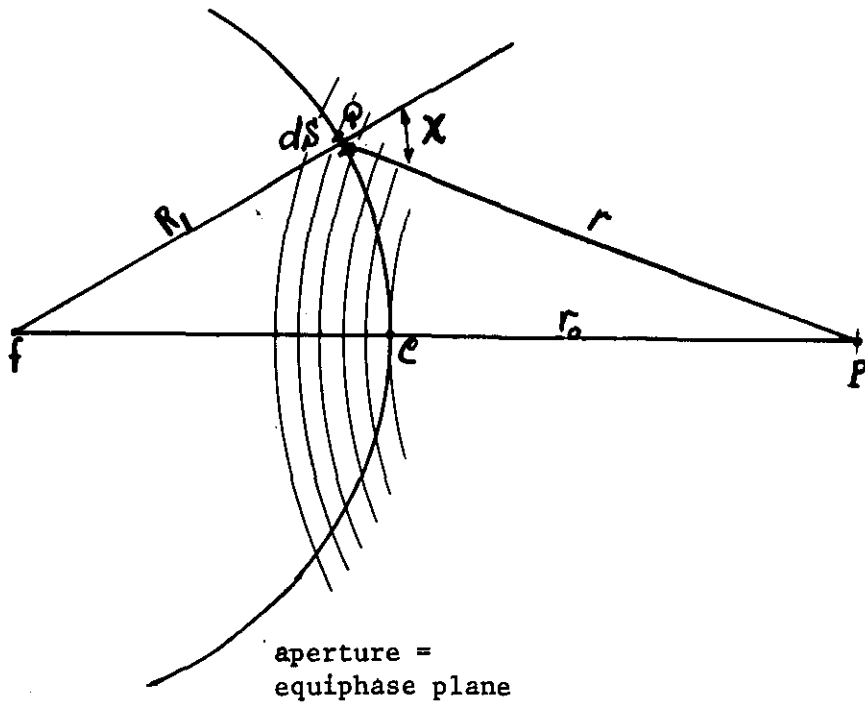certain requirements (ref. 6, Ch. 4):

Fig. 3.5

The Huygens Fresnel principle with C being a point of stationary phase

1. P should bot be situated in a focus or a focal plane.

2. P should not be situated at an optical shadow boundary.

3. The primary wavefront of the aperture may locally be regarded
   as plane, which means that $R_1 \gg \frac{1}{2}\lambda$.

4. The secondary wavefront at P should locally be plane as well,
   i.e. $r_o \gg \frac{1}{2}\lambda$.

In Fig. 3.5 spheres have been constructed with the centre at P
and with radii r_o, $r_o + \frac{1}{2}\lambda$, $r_o + 2x\frac{1}{2}\lambda$, etc. The lines intersecting
the aperture plane form the zones of Fresnel. The field contribution
dU (ref. 17, Ch. 8) due to the element dS at Q is:

$$dU\,(P) = K(\chi)\,U_o\,\frac{e^{-jkR_1}}{R_1} \cdot \frac{e^{-jkr}}{r}\,dS \quad , \qquad\qquad (3.14)$$

where U_o is a constant and $K(\chi)$ an inclination factor describing the variation with direction of the amplitude of the secondary waves with χ, χ being the angle of diffraction. The maximum of K is found in the original direction of propagation for $\chi = 0$, and $K = 0$ for $\chi = \frac{\pi}{2}$.

The total field at P is given by

$$U_P = U_o \frac{e^{-jkR_1}}{R_1} \iint_A \frac{e^{-jkr}}{r} K(\chi) \, dS , \qquad (3.15)$$

A being the aperture plane.

Eq.(3.15) may be evaluated using the zone construction of Fresnel. The contribution of n Fresnel zones can be approximated by (ref.17)

$$U_P \approx \tfrac{1}{2} \left[U_1 \, (P) + U_n \, (P) \right] \qquad (3.16)$$

where

$$U_n \, (P) = 2j\lambda U_o \frac{e^{-jk(R_1+r_o)}}{R_1 + r_o} (-1)^{n+1} K_n \quad . \qquad (3.17)$$

For the last zone χ approaches to $\frac{\pi}{2}$, where the values of K become very small, therefore U_n is neglected with respect to U_1, thus Eq. (3.16) becomes

$$U_P \approx \tfrac{1}{2} U_1 \, (P) \qquad (3.18)$$

The field is apparently mainly determined by the half of the first Fresnel zone, which is concentrated in an area around C. This point is often called a point of stationary phase (ref. 6, p. 119); the phase of e^{-jkr} varies very slowly in the neighbourhood of such a point.

3.5 Final conclusions

By means of the theory of the preceding section we are now capable to judge whether the approximations announced in section 3.3 are correct. If we take, for example, a conical horn (Fig. 3.3) with $\alpha=30^\circ$,

$r_o = b = 12\lambda$ (meaning that $D = 12\lambda$ and $kb = 75$), and if we take
the fieldpoint under discussion at a distance $R = 22\lambda$ from the
aperture, we have an average horn, and are able to compare our
results with those of Li and Turrin (ref. 13).
In the point of stationary phase C (Fig. 3.5) we find that

$$\bar{E}_A \cdot \bar{i}_r = \bar{E}_A \cdot \bar{n} = 0 \tag{3.19}$$

and

$$\bar{E}_A (1 + \bar{n} \cdot \bar{i}_r) = 2 \bar{E}_A \tag{3.20}$$

since E_A is a tangent to the aperture and $E_A \perp \bar{n}$.
In the vicinity of C also

$$\left| (\bar{E}_A \cdot \bar{i}_r) \cdot (\bar{n} + \bar{i}_r) \right| << \left| \bar{E}_A (1 + \bar{n} \cdot \bar{i}_r) \right|. \tag{3.21}$$

We will now prove that the contribution of the entire aperture field
to E_p is mainly determined by the stationary points C so that
in Eq. (3.12) $(\bar{E}_A \cdot \bar{i}_r)(\bar{n} + \bar{i}_r)$ can be neglected with respect to
$\bar{E}_A \cdot (1 + \bar{n} \cdot \bar{i}_r)$.
We will assume that the fields in the aperture are equal to the
TE_{11} mode of a circular waveguide with spherical wavefronts.
According to Section 2.8 these fields are given by

$$E_\rho = j\omega\mu \cdot \frac{J_1(\kappa'_{11} \cdot \rho) \sin m\phi}{\rho} \tag{3.22}$$

and

$$E_\phi = j\omega\mu\kappa'_{11} J'_1 (\kappa'_{11}\rho) \cos m\phi \tag{3.23}$$

The amplitude over the aperture varies slowly with Θ_1, $J'_1 (x)$
being of the form $\cos x$ and $\frac{1}{x} J_1(x)$ of the form $\frac{\sin x}{x}$. In the
H plane for $\Theta_1 = \alpha$ the amplitude becomes zero. The direction
of polarisation is mainly in the y direction for those parts
of the aperture where E_A is largest.

$\alpha = 30^o$

$b = 12\lambda$

$R = 22\lambda$

$\Theta = 0^o \text{ and } 30^o$
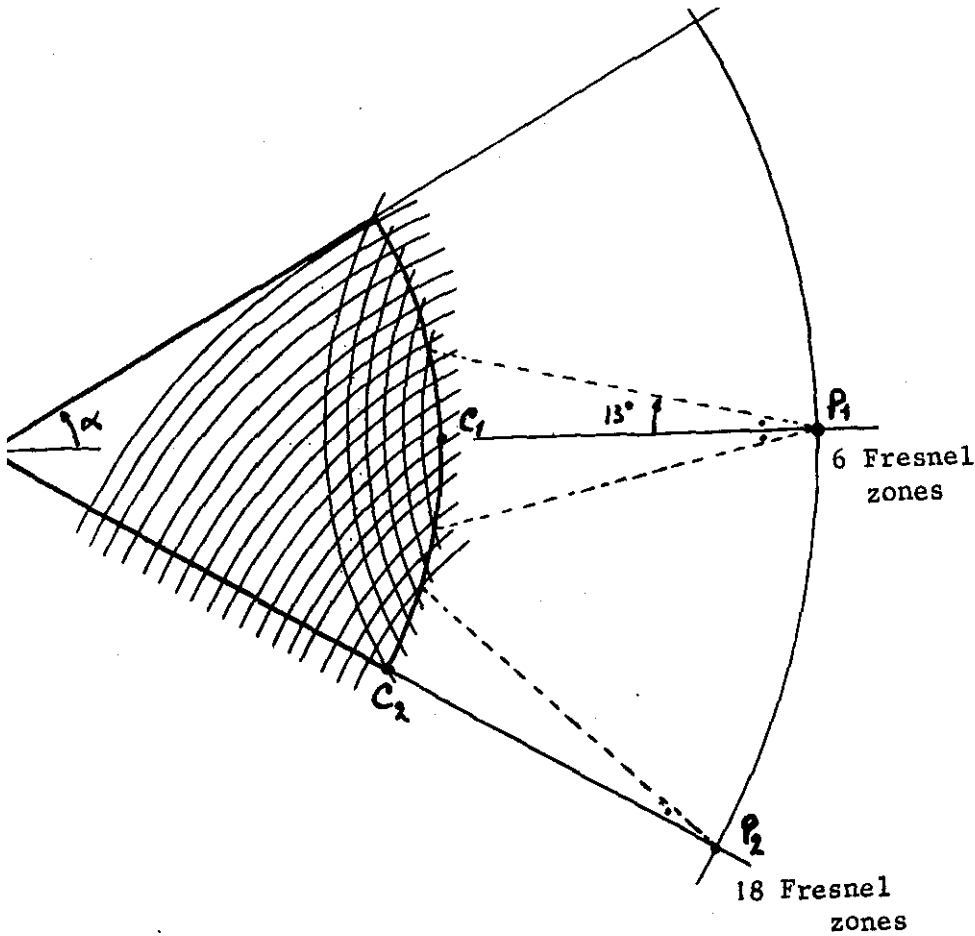
Fig. 3.6

Field approximations by Fresnel zones

We will now study the points P_1 and P_2 of Fig. 3.6; both meet the requirements for geometrical optical methods as stated in Section 3.4. For the first Fresnel zone we may approach $\bar{n} \approx \bar{i}_r$. The other Fresnel zones lie close to each other, so that contributions of adjacent zones will be cancelled. Moreover, the amplitude in the H plane decreases nearer to the aperture's edge. Therefore, we may conclude that the Huygens-Fresnel principle gives a satisfactory first approach and may use the approximations 3.21. For the points P_1 on the axis of the conical horn we may, therefore, use the equation

$$E_p = \frac{jk}{4\pi} \iint_A \bar{E}_A \, (1 + \bar{n}.\bar{i}_r) \, \frac{e^{-jkr}}{r} \, dS \, . \tag{3.24}$$

The fieldpoints P_2 are chosen in such a way that $\Theta \approx \alpha$ but $\Theta < \alpha$, which means that P_2 also meets the requirements of section 3.4. Therefore, the assumptions made for P_1 also apply to P_2. The approximations for P_2 are less correct than those for P_1 as the adjacent Fresnel zones for P_2 points are not symmetrical. It is also found from a point of view of geometrical optics that propagation is strongest in the n direction and zero when perpendicular to n, so that the area around the stationary points is most important.

Therefore, and keeping in mind the approximations of Sec. 3.4, for all points P where $\Theta < \alpha$ it is permissible to use Eq.(3.20). Apparently this equation when used for the entire aperture gives similar results in case that integration is only carried out over half the first Fresnel zone.

Measurements have been carried out by Li and Turrin (ref. 13) and it is noticed that the results correspond very reasonably with the theory.

4. Literatuur

1. Harrington R.F.:

   "Time harmonic electromagnetic fields",

   McGraw-Hill Book Company, New York, 1961.

2. Barrow W.L. and Chu L.J.:

   "Theory of the electromagnetic horn",

   Proc. IRE, pp. 51-64, Jan. 1939.

3. Schorr M.G. and Beck F.J.:

   Electromagnetic field of the conical horn",

   Journal of applied Physics, vol. 21, pp. 795-801, Aug. 1950.

4. Bucholtz H.:

   "Die Bewegung elektromagnetischer Wellen in einem Kegelförmigen Horn",

   Annalen der Physik, Band 37, pp. 173-225, Febr. 1940.

5. Abramowitz M.A. and Stegun J.A.:

   "Handbook of mathematical functions",

   Dover Publications, New York, 1965.

6. Silver S.:

   "Microwave antenna theory and design",

   McGraw-Hill Book Company, New York, 1949.

7. Geyer H.:

   "Runder Hornstrahler mit ringförmigen Sperrtöpfen zur gleichzeitigen

   Uebertragung zweier polarisationskoppelter Wellen".

   Frequenz, Bd. 20, nr. 1, pp. 22-28, Jan. 1966.

8. Lamont H.R.L.:

   "Waveguides",

   Methuen monographs on physical subjects,

   London, 1949.

9. Watson G.N.:

   "A treatise on the theory of Besselfunctions",

   Cambridge University Press, Cambridge, 1958.

10. Whittaker E.T. and Watson G.N.:
    "A course of modern analysis",
    Cambridge University Press, Cambridge, 1952.

11. Jones D.S.:
    "The theory of electromagnetism",
    Pergamon Press Ltd., Oxford, 1964.

12. Piefke G.:
    "Reflection at incidence of an H_{mn} wave at junction of circular
    waveguide and conical horn",
    Electromagnetic theory and antennas, pp. 209-234,
    Pergamon Press, Oxford, 1963.

13. Tingye Li and Turrin R.H.:
    "Near-Zone field of the conical horn",
    IEEE Transactions on Antennas and Propagation, pp. 800-802, Nov. 1964.

14. Zucker H., Ierley W.H.:
    "Computer aided analysis of Cassegrain antennas",
    Bell System Techn. Journal, pp. 897-932, July-Aug. 1968.

15. Cook J.S., Elam E.M. and Zucker H.:
    "The open Cassegrain antenna",
    Bell System Technical Journal, pp. 1255-1300, Sept. 1965.

16. Schelkunoff S.A.:
    "On diffraction and radiation of electromagnetic waves",
    Physical Review, pp. 308-316, Aug. 1939.

17. Born M. and Wolf E.:
    "Principles of Optics",
    Pergamon Press, Oxford, 1964.

18. Bodmer M.H :
    "Private Communication", 1969.

19. Koop H.E.M.:
    Report Graduate Work, T.H. Eindhoven, January 1969.

APPENDIX A

Coordinate transformations

(1) Transformation of rectangular coordinates into cylindrical coordinates,

$$
\begin{pmatrix} \bar{i}_x \\ \bar{i}_y \\ \bar{i}_z \end{pmatrix} = \begin{pmatrix} \cos\phi & -\sin\phi & 0 \\ \sin\phi & \cos\phi & 0 \\ 0 & 0 & 1 \end{pmatrix} \begin{pmatrix} \bar{i}_\rho \\ \bar{i}_\phi \\ \bar{i}_z \end{pmatrix}
$$

(2) Transformation of rectangular coordinates into spherical coordinates,

$$
\begin{pmatrix} \bar{i}_x \\ \bar{i}_y \\ \bar{i}_z \end{pmatrix} = \begin{pmatrix} \sin\Theta\cos\phi & \cos\Theta\cos\phi & -\sin\phi \\ \sin\Theta\sin\phi & \cos\Theta\sin\phi & \cos\phi \\ \cos\Theta & -\sin\Theta & 0 \end{pmatrix} \begin{pmatrix} \bar{i}_r \\ \bar{i}_\Theta \\ \bar{i}_\phi \end{pmatrix}
$$

(3) Transformation of cylindrical coordinates into spherical coordinates,

$$
\begin{pmatrix} \bar{i}_\rho \\ \bar{i}_\phi \\ \bar{i}_z \end{pmatrix} = \begin{pmatrix} \sin\Theta & \cos\Theta & 0 \\ 0 & 0 & 1 \\ \cos\Theta & -\sin\Theta & 0 \end{pmatrix} \begin{pmatrix} \bar{i}_r \\ \bar{i}_\Theta \\ \bar{i}_\phi \end{pmatrix}
$$

The symbols $\bar{i}$, used throughout this Appendix, indicate that only unit vectors have been employed.
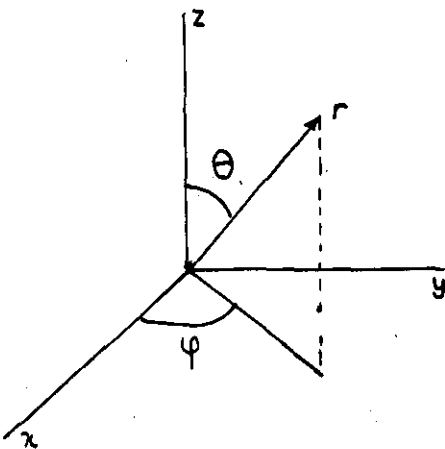
Fig. A1

Spherical coordinates
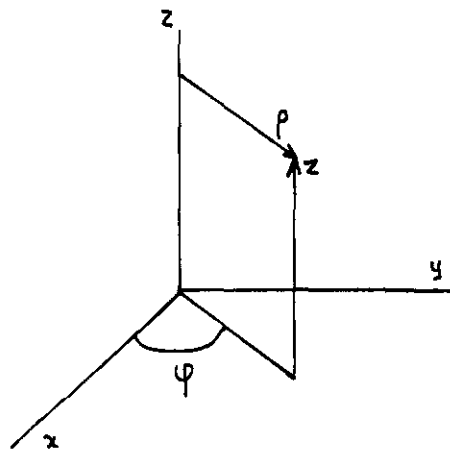
Fig. A2

Cylindrical coordinates

APPENDIX B

Vector Analysis

Below are some important vector equations in spherical coordinates, which have been used throughout this report.

$$\nabla a = \frac{\partial a}{\partial r} \bar{i}_r + \frac{1}{r} \frac{\partial a}{\partial \Theta} \bar{i}_\Theta + \frac{1}{r \sin \Theta} \frac{\partial a}{\partial \phi} \bar{i}_\phi \qquad (B.1)$$

$$\nabla \cdot \bar{A} = \frac{1}{r^2} \frac{\partial}{\partial r} (r^2 A_r) + \frac{1}{r \sin \Theta} \frac{\partial}{\partial \Theta} (A_\Theta \sin \Theta) + \frac{1}{r \sin \Theta} \frac{\partial A_\phi}{\partial \phi} \qquad (B.2)$$

$$\nabla \times \bar{A} = \frac{1}{r \sin \Theta} \left[\frac{\partial}{\partial \Theta} (A_\phi \sin \Theta) - \frac{\partial A_\Theta}{\partial \phi} \right] \bar{i}_r +$$
$$+ \frac{1}{r} \left[\frac{1}{\sin \Theta} \frac{\partial A_r}{\partial \phi} - \frac{\partial}{\partial r} (r A_\phi) \right] \bar{i}_\Theta + \frac{1}{r} \left[\frac{\partial}{\partial r} (r A_\Theta) - \frac{\partial A_r}{\partial \Theta} \right] \bar{i}_\phi \qquad (B.3)$$

$$\nabla^2 a = \Delta a = \frac{1}{r^2} \frac{\partial}{\partial r} (r^2 \frac{\partial a}{\partial r}) + \frac{1}{r \sin \Theta} \frac{\partial}{\partial \Theta} (\sin \Theta \frac{\partial a}{\partial \Theta}) + \frac{1}{r^2 \sin^2 \Theta} \frac{\partial^2 a}{\partial \phi^2} \qquad (B.4)$$

$$\nabla (\frac{1}{r} e^{-jkr}) = (jk + \frac{1}{r}) \frac{1}{r} e^{-jkr} \bar{i}_r \qquad (B.5)$$

$$(\bar{A} \cdot \nabla) \nabla (\frac{1}{r} e^{-jkr}) = \left[-k^2 (\bar{A} \cdot \bar{i}_r) \bar{i}_r + \frac{3}{r} (jk + \frac{1}{r}) (\bar{A} \cdot \bar{i}_r) \bar{i}_r - \frac{\bar{A}}{r} (jk + \frac{1}{r}) \right] \frac{1}{r} e^{-jkr}$$

$$(B.6)$$

APPENDIX C

Bessel Functions

1. Introduction

In this Appendix only those properties and relations with Bessel
functions will be discussed in dealing with the problems and
theory of Chapter 2.
More about Bessel functions are to be found in various handbooks
(refs. 5, 9, 10).
The Bessel equation of integer order ν is represented by

$$z^2 w'' + 2w' + (z^2 - \nu^2)w = 0,$$ (C.1)

with solutions of the first kind $J_\nu(z)$ and $J_{-\nu}(z)$, of the second
kind $Y_\nu(z)$ (also called Neumann or Weber functions). The solutions
of the third kind, known as Hankel functions, are related to the
previous ones by

$$H_\nu^{(1)}(z) = J_\nu(z) + j\, Y_\nu(z)$$
$$H_\nu^{(2)}(z) = J_\nu(z) - j\, Y_\nu(z)$$ (C.2)

The solutions of the Bessel functions are represented in Figs.C1-C6;
some properties of them are very important.
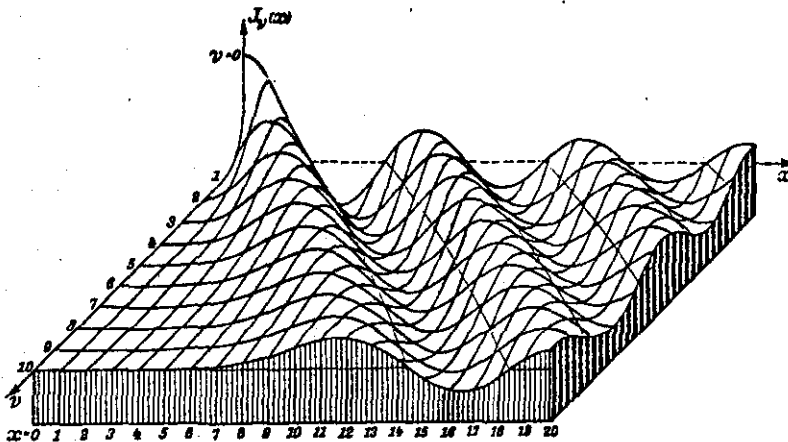
Fig. C1

$J_\nu(x)$
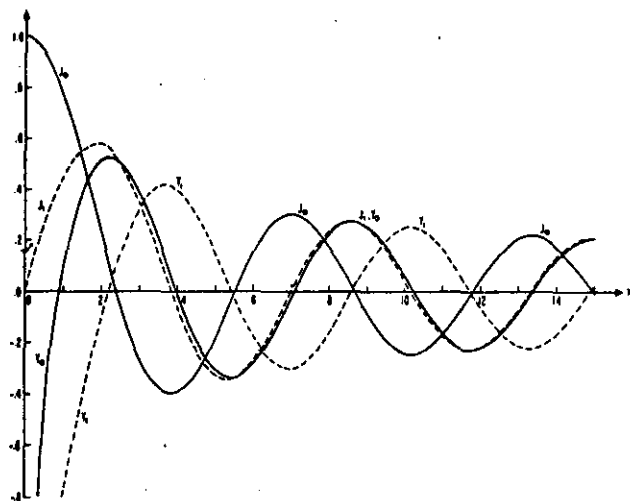
Fig. C_2. $J_0(x)$, $Y_0(x)$, $J_1(x)$, $Y_1(x)$.
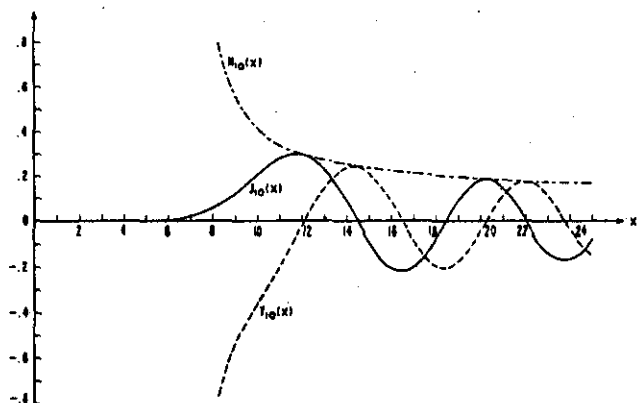
Fig. C_3. $J_{10}(x)$, $Y_{10}(x)$, and $M_{10}(x) = \sqrt{J_{10}^2(x) + Y_{10}^2(x)}$.

Fig. C_4: $J_\nu^-(10)$ and $Y_\nu(10)$.
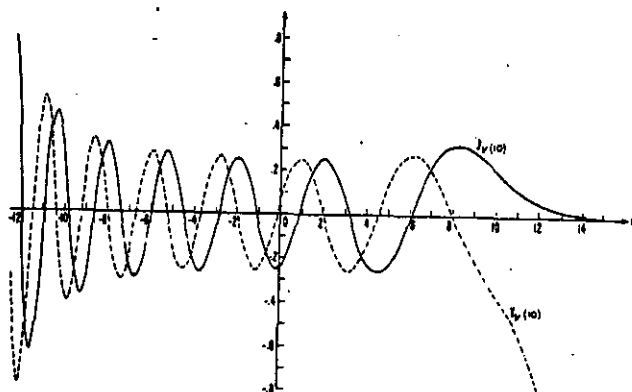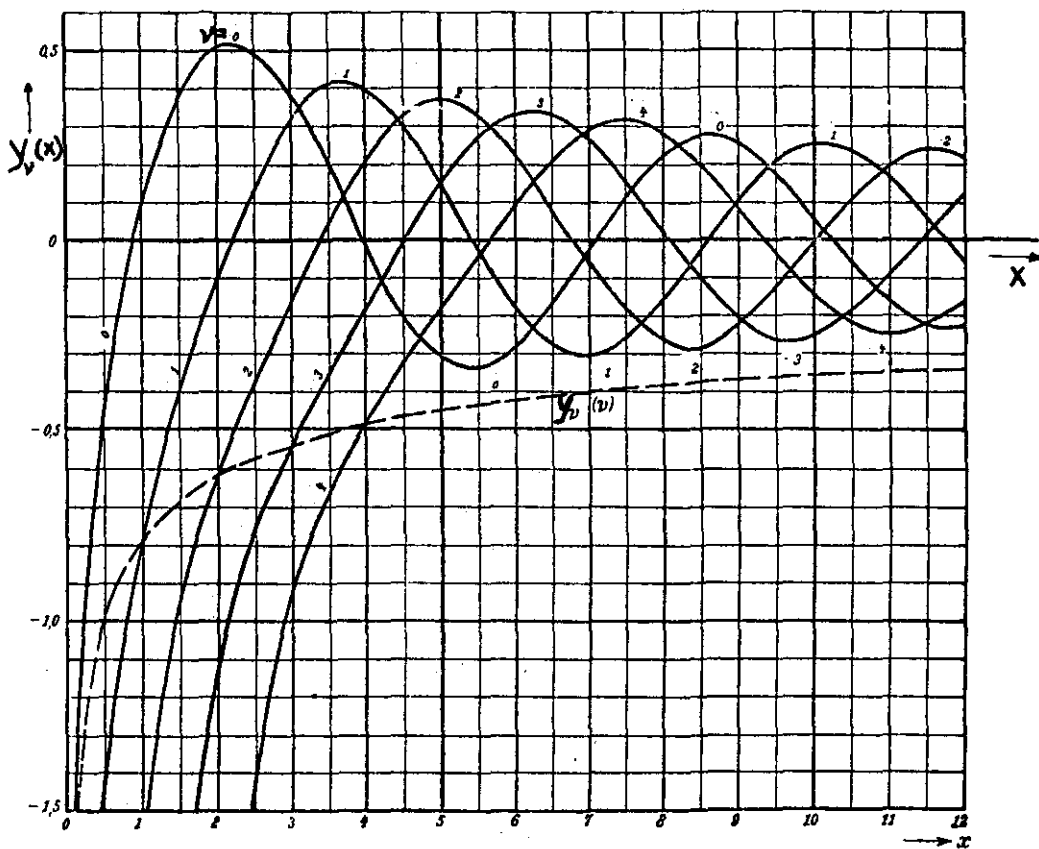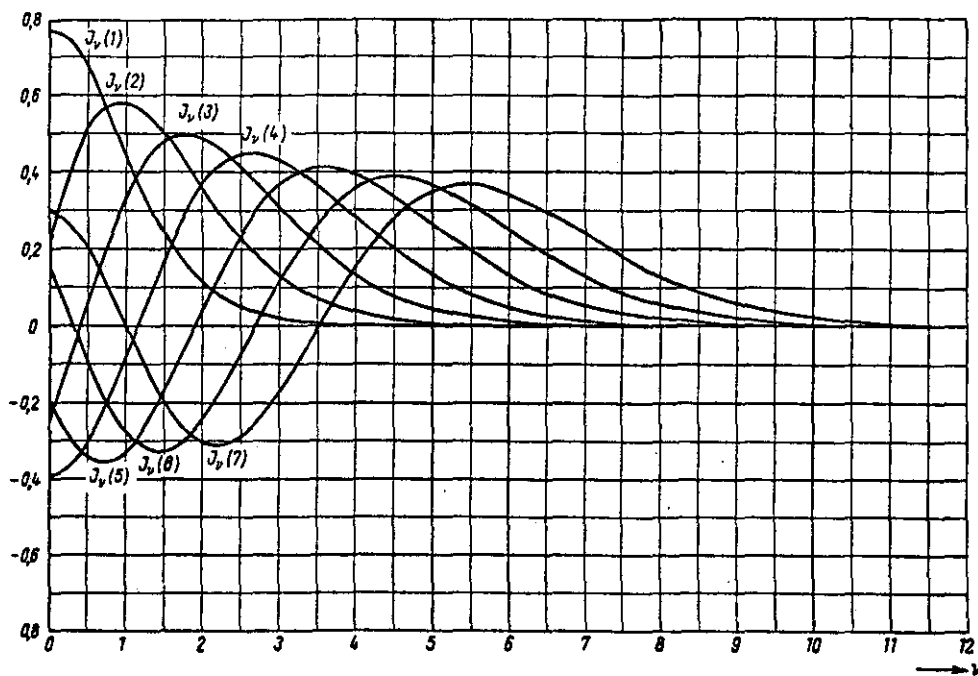
Fig. C_5: $Y_\nu(x)$, ν being a parameter.

Fig. C_6: $J_\nu(x)$, x being a parameter.

Solutions of the first kind $J_\nu(x)$ are finite for all values of x.
Solutions of the second kind $Y_\nu(x)$ are finite for x $\neq$ 0 and for
x = 0 equal to $-\infty$. For $\nu \geq 0$, $J_\nu(x)$ is limited for all values
of x and $Y_\nu(x)$ will be $-\infty$ for large ν.

2. Limiting forms and relations

2.1 Limiting forms for small arguments

For x $\to$ 0 and ν fixed (ref. 5, 9.1.7)

$$J_\nu(x) \approx \left(\frac{x}{2}\right)^\nu \frac{1}{\Gamma(\nu+1)} \; ; \quad \nu \neq -1, -2, -3, \ldots \tag{C.3}$$

$$Y_\nu(x) \approx -j \, H_\nu^{(1)}(x) \approx j \, H_\nu^{(2)}(x) \approx -\frac{1}{\pi} \, \Gamma(\nu) \left(\frac{2}{x}\right)^\nu ; \quad \nu \geq 0 \tag{C.4}$$

2.2 Asymptotic expansions for large orders

If $\nu \to \infty$ through positive values and all other variables remain
fixed (ref. 5, 9.3.1) then

$$J_\nu(x) \approx \frac{1}{\sqrt{2\pi\nu}} \left(\frac{ex}{2\nu}\right)^\nu \tag{C.5}$$

$$Y_\nu(x) \approx -\sqrt{\frac{2}{\pi\nu}} \left(\frac{ex}{2\nu}\right)^{-\nu} \tag{C.6}$$

2.3 Relations between solutions (ref. 5, 9.1.5 etc.)

$$J_{-n}(x) = (-1)^n \, J_n(x) \tag{C.7}$$

$$Y_{-n}(x) = (-1)^n \, Y_n(x) \tag{C.8}$$

2.4 Recurrence relations (ref. 5, 9.1.27)

If $B_\nu(x)$ denotes an arbitrary solution of the Bessel equation with
integer order, then

$$\frac{2\nu}{x} B_\nu(x) = B_{\nu-1}(x) + B_{\nu+1}(x) \tag{C.9}$$

$$2 B_\nu'(x) = B_{\nu-1}(x) - B_{\nu+1}(x) \tag{C.10}$$

$$B_\nu'(x) = B_{\nu-1}(x) - \frac{\nu}{x} B_\nu(x) \tag{C.11}$$

$$B_\nu'(x) = \frac{\nu}{x} B_\nu(x) - B_{\nu+1}(x) \tag{C.12}$$

2.5 Generating functions (ref. 5, 9.1.44, etc.)

$$\cos(x \cos \phi) = J_0(x) + 2 \sum_{k=1}^{\infty} (-1)^k J_{2k}(x) \cos(2k\phi) \tag{C.13}$$

$$\sin(x \cos \phi) = 2 \sum_{k=\nu}^{\infty} (-1)^k J_{2k+1}(x) \cos\{(2k + 1)\phi\} \tag{C.14}$$

2.6 Asymptotic expansions for large arguments (ref. 5, 9.2.1)

If ν is fixed and $x \to \infty$ then

$$J_\nu(x) = \sqrt{\frac{2}{\pi x}} \cos\left(x - \frac{2\nu + 1}{4}\pi\right) + 0\left(\frac{1}{x}\right) \tag{C.15}$$

$$Y_\nu(x) = \sqrt{\frac{2}{\pi x}} \sin\left(x - \frac{2\nu + 1}{4}\pi\right) + 0\left(\frac{1}{x}\right) \tag{C.16}$$

$$H_\nu^{(1)}(x) = \sqrt{\frac{2}{\pi x}} \exp\left[j\left(x - \frac{2\nu + 1}{4}\pi\right)\right] + 0\left(\frac{1-j}{x}\right) \tag{C.17}$$

$$H_\nu^{(2)}(x) = \sqrt{\frac{2}{\pi x}} \exp\left[-j\left(x - \frac{2\nu + 1}{4}\pi\right)\right] + 0\left(\frac{1-j}{x}\right) , \tag{C.18}$$

where a series $\sum_{k=0}^{\infty} a_k x^{-k}$ is said to be an asymptotic expansion of a function $f(x)$,

if

$$f(x) - \sum_{k=0}^{n-1} a_k x^{-k} = 0(x^{-n}) \text{ if } x \to \infty. \tag{C.19}$$

We write

$$f(x) \sim \sum_{k=0}^{\infty} a_k x^{-k} . \tag{C.20}$$

The series itself may either be convergent or divergent (ref. 5, 3.6.15).

2.7 Zeros [Ref. 5, 9.5.12]

If ν remains fixed and $s \gg \nu$, the sth zero-point of the Bessel solutions $\varepsilon_{\nu,s}$ of $J_\nu(x)$ and $\sigma'_{\nu s}$ of $Y'(x)$ are $(s + \frac{1}{2}\nu - \frac{1}{4})\pi$.
The zero-points $\varepsilon'_{\nu,s}$ of $J'_\nu(x)$ and $\sigma_{\nu,s}$ of $Y_\nu(x)$ are

$$(s + \frac{1}{2}\nu - \frac{3}{4})\pi \qquad (C.22)$$

The first positive zero-point in these solutions will be found for s=1, with the exception that the first zero-point $\varepsilon'_{0,1}$ of $J'_0(x)$ will be zero.
The expansions give a very good approximation also for small values $s > \nu$.
This feature is a well-known property of asymptotic expansions.

3. Bessel functions of fractional order

3.1 Introduction

The Bessel differential equation

$$z^2 w'' + 2zw' + \left[z^2 - n(n+1)\right] w = 0 , \qquad (C.23)$$
$$\text{where } n=0, \pm 1, \pm 2, \ldots,$$

has particular solutions, namely spherical Bessel functions of the first kind:

$$j_n(z) = \sqrt{\frac{\pi}{2z}} \ J_{n+\frac{1}{2}}(z) , \qquad (C.24)$$

of the second kind

$$y(z) = \sqrt{\frac{\pi}{2z}} \ Y_{n+\frac{1}{2}}(z) \qquad (C.25)$$

and of the third kind

$$h_n^{(1)}(z) = j_n(z) + jy_n(z)$$

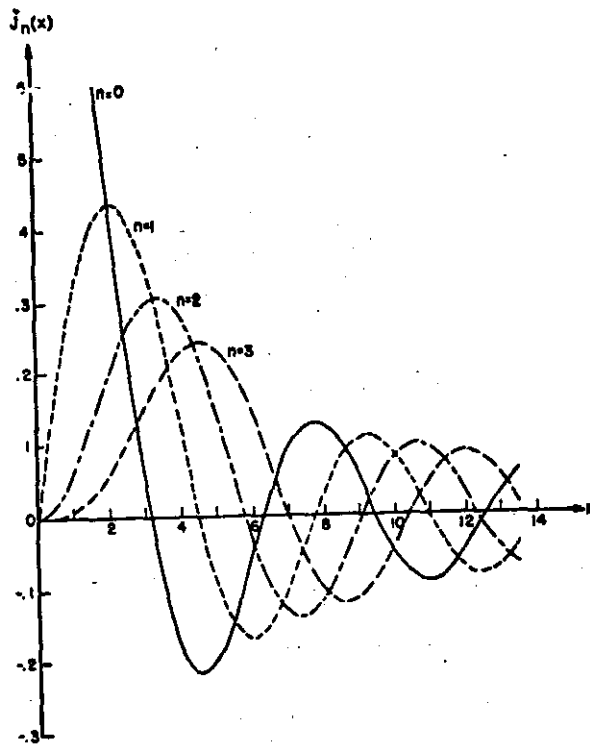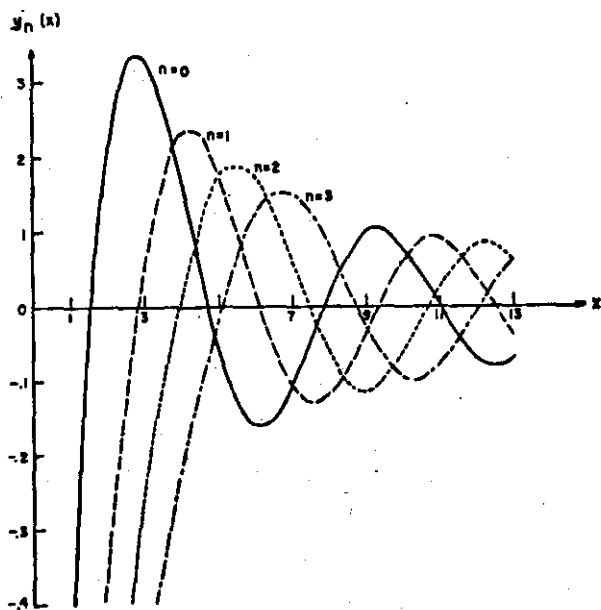$$h_n^{(2)}(z) = j_n(z) - jy_n(z) \qquad (C.26)$$

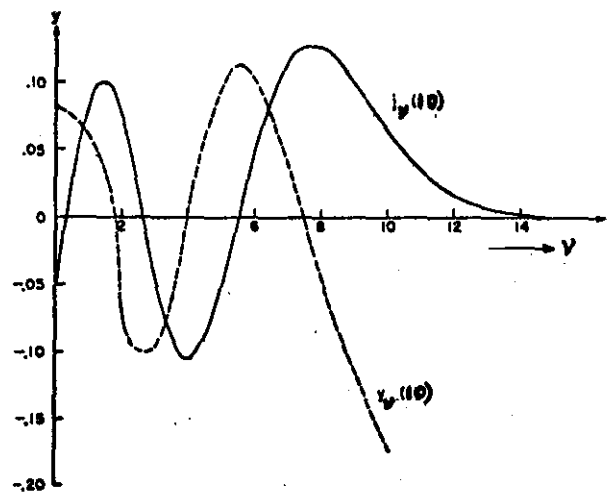Fig.C_7: $j_n(x)$.

Fig.C_8: $y_n(x)$.

Fig. C_9: $j_\nu(10)$ and $y_\nu(10)$.

or for arbitrary solutions (See also Figs. C7 - C9)

$$b_\nu(z) = \sqrt{\frac{\pi}{2z}} \ B_{\nu+\frac{1}{2}}(z) \ .$$

(C.27)

3.2 Limiting values as $x \to 0$ (ref. 5, 10.1.4)

$$\left. \begin{array}{l} j_n(x) \to x^n \cdot \dfrac{1}{1 \cdot 3 \cdot 5 \cdot \ \ldots \ (2n+1)} \\[3mm] y_n(x) \to \dfrac{1}{x^{n+1}} \left[1 \cdot 3 \cdot 5 \cdot \ \ldots \ (2n-1) \right] \end{array} \right\} \ n = 0, \ 1, \ 2, \ \ldots$$

(C.28)

$$y_n(-x) \to (-1)^{n+1} j_{-1-n}(x) \ ; \quad n = 0, \ \pm 1, \ \pm 2, \ \ldots \quad .$$

(C.29)

(ref. 5, 10.1.15).

3.3 Recurrent relations (ref. 5, 10.1.19).

$$\frac{2\nu + 1}{x} \ b_\nu(x) = b_{\nu-1}(x) + b_{\nu+1}(x)$$

(C.30)

$$(2\nu+1)b_\nu'(x) = \nu b_{\nu-1}(x) - (\nu+1)b_{\nu+1}(x)$$

(C.31)

$$b_\nu'(x) = b_{\nu-1}(x) - \frac{\nu+1}{x} b_\nu(x)$$

(C.32)

$$b_\nu'(x) = \frac{\nu}{x} b_\nu(x) - b_{\nu+1}(x)$$

(C.33)

3.4 The function $h_\nu^{(2)}(x)$

Following Eq. (C.27) we may write

$$h_\nu^{(2)}(x) = \sqrt{\frac{\pi}{2x}} \ H_{\nu+\frac{1}{2}}^{(2)}(x).$$

(C.34)

With Eq. (C.18) we obtain for large x

$$h_\nu^{(2)}(x) = \frac{1}{x} \left[j \exp \left[-j(x - \frac{\nu}{2}\pi) \right] + O(\frac{1-j}{x\sqrt{x}}) \right].$$

(C.35)

For large values of ν we find, using the Eqs. (C.23, C.24, C.25) and Eqs. (C.5 and C.6)

$$h_\nu^{(2)}(x) = \sqrt{\frac{\pi}{2x}} \left[J_{\nu+\frac{1}{2}}(x) - jY_{\nu+\frac{1}{2}}(x) \right] \sim$$

$$\sim \sqrt{\frac{\pi}{2x}} \quad \frac{1}{\sqrt{2\pi(\nu+\frac{1}{2})}} \cdot \left\{ \left(\frac{ex}{2\nu+1}\right)^{\nu+\frac{1}{2}} + 2j\left(\frac{2\nu+1}{ex}\right)^{\nu+\frac{1}{2}} \right\}$$

or

$$h_\nu^{(2)}(x) \sim \frac{1}{\sqrt{2x(2\nu+1)}} \cdot \left[\left(\frac{ex}{2\nu+1}\right)^{\nu+\frac{1}{2}} + 2j\left(\frac{2\nu+1}{ex}\right)^{\nu+\frac{1}{2}} \right] \qquad (C.36)$$

To obtain a better insight into the function $h_\nu^{(2)}(x)$ we will first study the behaviour of the function $H_{\nu+\frac{1}{2}}^{(2)}(x)$. To this end we write

$$H_{\nu+\frac{1}{2}}^{(2)}(x) = M_{\nu+\frac{1}{2}} \exp\left(-j\Theta_{\nu+\frac{1}{2}}\right) \qquad (C.37)$$

where $M_{\nu+\frac{1}{2}} = \left| H_{\nu+\frac{1}{2}}^{(2)}(x) \right|$ and $\Theta_{\nu+\frac{1}{2}} = \mathrm{Arg}\, H_{\nu+\frac{1}{2}}(x)$.

According to Abramowitz (ref. 5, 9.2.28) we find for $\nu = $ constant and large x:

$$M_\nu \sim \sqrt{\frac{2}{\pi x}} \left[1 + \frac{1}{2} \cdot \frac{4\nu^2 - 1}{(2x)^2} + \ldots \right]^{\frac{1}{2}} \quad , \qquad (C.38)$$

and

$$\Theta_\nu \sim x - \frac{2\nu+1}{4}\pi + \frac{4\nu^2 - 1}{8x} + \ldots \qquad (C.39)$$

Eqs. (C.38) and (C.39) yield

$$M_{\nu+\frac{1}{2}} \sim \sqrt{\frac{2}{\pi x}} \left[1 + \frac{\nu(\nu+1)}{2x^2} + \ldots \right]^{\frac{1}{2}} \qquad (C.40)$$

$$\Theta_{\nu+\frac{1}{2}} \sim x - \frac{\nu+1}{2}\pi + \frac{\nu(\nu+1)}{2x} \qquad (C.41)$$

It is a well-known property of asymptotic expansions that the function is very well approximated for large values of x. By the first term of the expansion we may, therefore, conclude that for $x > \nu$

$$M_{\nu+\frac{1}{2}} \rightarrow \left(\frac{2}{\pi x}\right)^{\frac{1}{2}} \tag{C.42}$$

and

$$\Theta_{\nu+\frac{1}{2}} \rightarrow x - \frac{\nu + 1}{2} \pi \tag{C.43}$$

(See also Fig. C10).

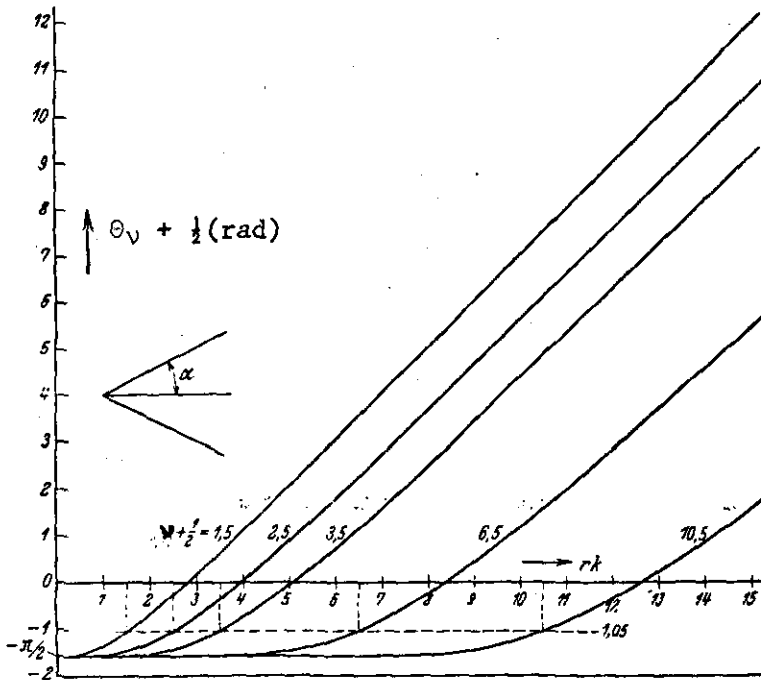This figure shows clearly that $\Theta_{\nu+\frac{1}{2}}$ varies linearly with x for $x > \nu$.

Fig. C10

3.5 The derivatives of the function $\hat{B}_\nu(x) = x \, b_\nu(x)$

From Eq. (C.32) we obtain, writing $b_\nu(x) = \frac{1}{x} \hat{B}_\nu(x)$,

$$-\frac{1}{x^2} \hat{B}_\nu(x) + \frac{1}{x} \hat{B}'_\nu(x) = \frac{1}{x} \hat{B}_{\nu-1}(x) - \frac{\nu + 1}{x^2} \hat{B}_\nu(x)$$

or $\qquad \hat{B}'_\nu(x) = \hat{B}_{\nu-1}(x) - \frac{\nu}{x} \hat{B}_\nu(x)$. $\qquad$ (C.44)

From Eq. (C.33) we obtain

$$\hat{B}'_\nu (x) = \frac{\nu + 1}{x} \cdot \hat{B}_\nu (x) - \hat{B}_{\nu+1} (x) \tag{C.45}$$

Eq. (C.44) now yields

$$\hat{B}''_\nu (x) = \frac{\partial}{\partial x} \left[\hat{B}_{\nu-1} (x) - \frac{\nu}{x} \hat{B}_\nu (x) \right]$$

$$= \hat{B}'_{\nu-1} (x) + \frac{\nu}{x^2} B_\nu (x) - \frac{\nu}{x} B'_\nu (x) \tag{C.45}$$

Substituting Eqs. C44 and C45 in Eq. C46 we obtain

$$\hat{B}''_\nu (x) = \left[\frac{\nu}{x} \hat{B}_{\nu-1} (x) - \hat{B}_\nu (x) \right] + \frac{\nu}{x^2} \hat{B}_\nu (x) - \frac{\nu}{x} \left[\hat{B}_{\nu-1} (x) - \frac{\nu}{x} B_\nu (x) \right]$$

$$= B_\nu (x) \left[-1 + \frac{\nu}{x^2} + \frac{\nu^2}{x^2} \right] \tag{C.46}$$

Hence,

$$\frac{\partial}{\partial x^2} \left[x \, b_\nu (x) \right] = x \, b_\nu \left[\frac{\nu(\nu + 1)}{x^2} - 1 \right] \tag{C.47}$$

3.6 **The function** $\dfrac{1}{x} + \dfrac{h_\nu^{(2)'} (x)}{h_\nu^{(2)} (x)}$

Using Eq. (C.27) we find for the derivative of the Hankel function of the third kind

$$h_\nu^{(2)'} (x) = \frac{\partial}{\partial x} \left[\sqrt{\frac{\pi}{2x}} \cdot H_{\nu+\frac{1}{2}}^{(2)} (x) \right]$$

$$= - \frac{1}{2x} \sqrt{\frac{\pi}{2x}} \cdot H_{\nu+\frac{1}{2}}^{(2)} (x) + \sqrt{\frac{\pi}{2x}} \cdot H_{\nu+\frac{1}{2}}^{(2)'} (x) \ . \tag{C.48}$$

As

$$h_\nu^{(2)} (x) = \sqrt{\frac{\pi}{2x}} H_{\nu+\frac{1}{2}}^{(2)} (x) \quad \text{it is readily seen that}$$

$$\frac{h_{\nu}^{(2)'}(x)}{h_{\nu}^{(2)} x} = -\frac{1}{2x} + \frac{H_{\nu+\frac{1}{2}}^{(2)'}(x)}{H_{\nu+\frac{1}{2}}^{2}(x)} \qquad \text{or}$$

$$\frac{1}{x} + \frac{h_{\nu}^{(2)'}(x)}{h_{\nu}^{(2)}(x)} = \frac{1}{2x} + \frac{H_{\nu+\frac{1}{2}}^{(2)'}(x)}{H_{\nu+\frac{1}{2}}^{(2)}(x)} \quad . \qquad \text{(C.49)}$$

In accordance with Abramowitz (ref. 5, 9.2.18) we will write

$$H_{\nu+\frac{1}{2}}^{(2)'}(x) = N_{\nu+\frac{1}{2}} \exp\left(-j \ \phi_{\nu+\frac{1}{2}}\right) \qquad , \text{ where}$$

ν is a constant and N real. Far large x we obtain the asymptotic expansions (ref. 5, 9.2.30).

$$N_{\nu+\frac{1}{2}} \sim \sqrt{\frac{2}{\pi x}} \ \left[1 - \frac{1}{2} \frac{\nu(\nu+1)}{x^2} + \frac{1}{4x^2} - \ldots\right]^{\frac{1}{2}} \qquad \text{(C.50)}$$

and

$$\phi_{\nu+\frac{1}{2}} \sim x - \frac{\nu}{2} \pi + \frac{\nu^2 + \nu + 1}{2x} + \ldots \qquad . \qquad \text{(C.51)}$$

If $x > \nu$ Eqs. (C.50) and (c.51) rapidly become

$$N_{\nu+\frac{1}{2}} \sim \sqrt{\frac{2}{\pi x}} \qquad \text{(C.52)}$$

$$\phi_{\nu+\frac{1}{2}} \sim x - \frac{\nu}{2} \pi \qquad . \qquad \text{(C.53)}$$

Using the results found for $H_{\nu+\frac{1}{2}}(x)$ (Eqs. (C.40) and (C.41)), it is readily seen that

$$\frac{H_{\nu+\frac{1}{2}}^{(2)'}}{H_{\nu+\frac{1}{2}}} \sim -j \qquad \text{(C.54)}$$

Therefore, if $x \gg 1$ and $x > \nu$

$$\frac{1}{x} + \frac{h_{\nu}^{(2)'}}{h_{\nu}^{(2)}} \approx -j \qquad . \qquad \text{(C.55)}$$

To obtain a better insight into the errors which have been made
in the approximations, the real and imaging parts of
$H(\nu,x) = H_\nu^{(2)'}/H_\nu^{(2)}$ are shown in Figs. C11 and C12 as a function
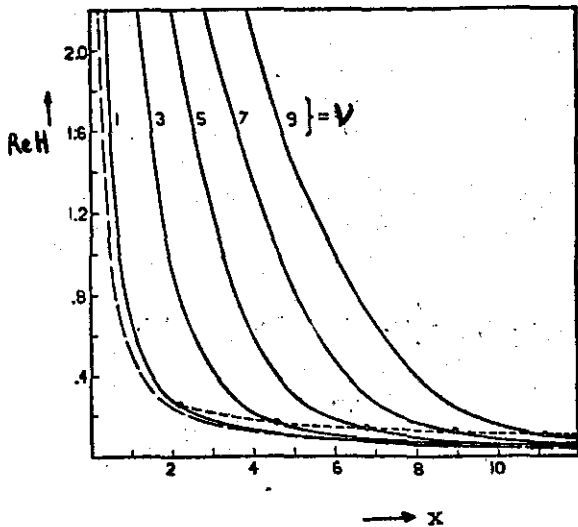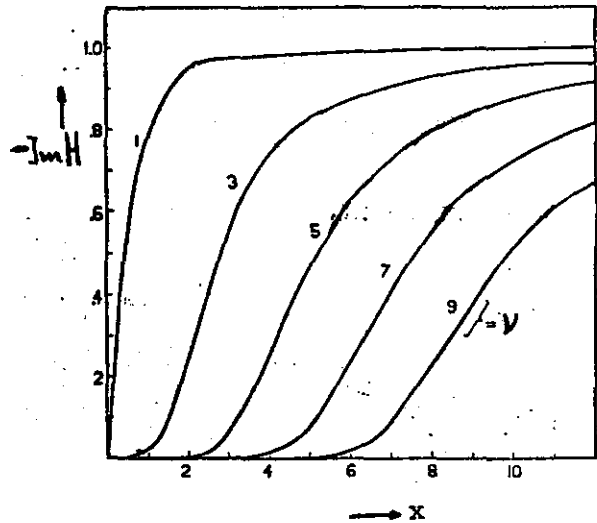of x, ν being a parameter (ref. 2).

Fig. C11

Fig. C12

Figs. C13 and C14 give the reprocal value of $H_{\nu,x}$ being

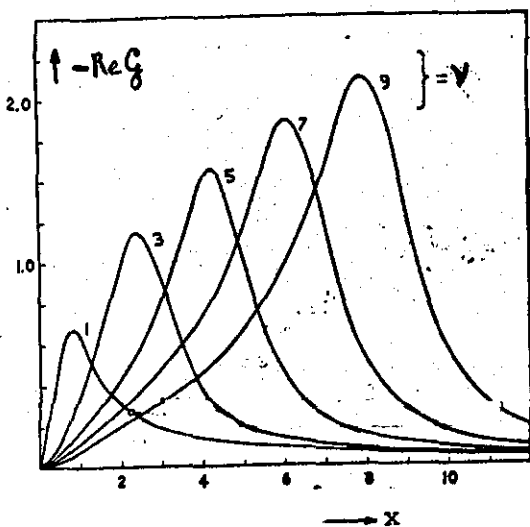$$G_{(\nu,x)} = \frac{1}{H_{(\nu,x)}}$$, which is important for $\nu \gg 1$.
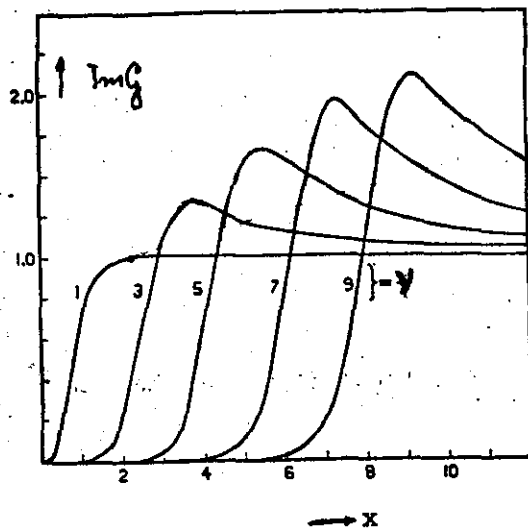
Fig. C13

Fig. C14

APPENDIX D

Legendre functions

1. Introduction

In this Appendix we shall mention some important properties of
Legendre functions as far as they are required to understand
Chapter 2 of the present report. Further properties of Legendre
functions are found in various handbooks and in some papers
(refs. 5, 10 .....).
We will employ Legendre functions only with real arguments x
which are found for $z \to x + j.0$.
The associated Legendre equation is

$$(1 - x^2)\, w'' - 2xw' + \left[\nu(\nu +1) - \frac{\mu^2}{1 - x^2} \right]\, w = 0 \qquad (D.1)$$

where $x = \cos \Theta$ is the argument and Θ likewise a real number;
ν is the degree and μ the order of the equation, and if $\mu = 0$
the equation is called Legendre equation.
The equation has solutions of the first kind $P_\nu^\mu (x)$ and of the
second kind $Q_\nu^\mu (x)$. We shall only discuss here solutions of the
first kind.
If ν is the non-negative integer n, P_n^μ is called a polynomial
of degree n, unless μ is a non-negative integer m. In this case
P_n^m is a polynomial of degree n–m, which vanishes identically
if m > n. The functions in which m=0 are known as Legendre
polynomials and written P_n (ref. 11, p.79).

2. Some properties and equations of Legendre functions

If $\mu = m$ (m = integer) and $x = \cos \Theta$, the solution of the first
kind (ref. 4) can be written

$$P_\nu^m (\cos \Theta) = (-1)^m .(1-x^2)^{m/2} . \frac{\Gamma(1+\nu+m)}{2^m \Gamma(1+\nu-m).\Gamma(1+m)} . F(m-\nu,\ m+\nu+1;\ m+1;\ \tfrac{1-x}{2})$$

$$(D.2)$$

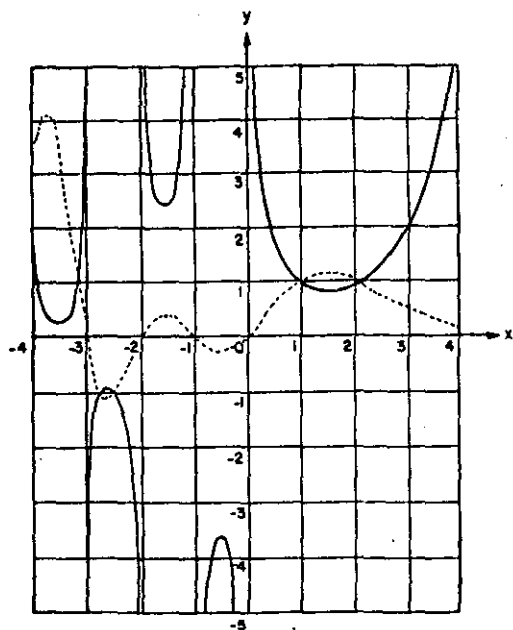In this equation Γ represents a gamma function (ref. 5, 6.1); see also Fig. D1.

Fig. D1.

$$— \;=\; \Gamma(x) \;=\; (x-1)! \;=\; \Pi(x-1)$$

$$\cdots \;=\; \frac{1}{\Gamma x}$$

The function F is the Gauss hypergeometric series (ref. 5, 15.1). The series converges for $|z| < 1$. In our case $z = \frac{1}{2}(1-x)$ and $\Theta < x \leq 1$ so that we meet the requirements of convergence. $P_\nu^m(x)$ is finite for $x = 1$. Further (ref.4, p.218).

$$P_\nu^{-m}(x) \;=\; (-1)^m \; \frac{\Gamma(\upsilon - m + 1)}{\Gamma(\upsilon + m + 1)} \; P_\nu^m(x) \; . \tag{D.3}$$

For small values of ν the following asymptotic expansion (ref.4,p.223) can be used

$$P_\nu^{-\mu}(\cos\,\Theta) = \left[\psi\right]^{-\mu}\left[J_\mu(\psi) + (\sin\,\tfrac{1}{2}\Theta)^2 \left\{\frac{1}{2\psi}\,J_{\mu+1}(\psi) - J_{\mu+2}(\psi) + \right.\right.$$

$$\left. + \frac{\psi}{6}\,J_{\mu+3}(\psi)\right\} + (\sin\,\tfrac{1}{2}\Theta)^4 \left\{\frac{9}{8\psi^2}\,J_{\mu+2}(\psi) - \frac{29}{6\psi}\,J_{\mu+3}(\psi) + \right.$$

$$\left.\left. + \frac{31}{12}\,J_{\mu+4}(\psi) - \frac{11}{30}\,\psi\cdot J_{\mu+5}(\psi) + \frac{\psi^2}{72}\,J_{\mu+6}\,\psi\right\} + O\{(\sin\,\tfrac{1}{2}\Theta)\}^6\right] \tag{D.4}$$

In Eq. (D.4) $\psi = (2\nu + 1)\,\sin\,\tfrac{1}{2}\Theta$ and

$$\psi' = (\nu + \tfrac{1}{2})\,\cos\,\tfrac{1}{2}\Theta \; .$$

It is further assumed that $\Theta \to 0$; $|\nu| \to \infty$; x is finite and $\neq 0$; μ and argument ν are arbitrary.

Jones (ref. 11, p.79) has shown that Eq. (D.4) can be simplified considerably to

$$P_\nu^{-\mu}(\cos \Theta) = (\psi') \, J_\mu \, (\psi) \left[1 + 0(\sin^2 \tfrac{1}{2}\Theta) \right] \tag{D.5}$$

The derivative of Eq. (D.5) gives

$$\frac{d}{d\Theta} \, P_\nu^{-\mu}(\cos \Theta) = - \sin \Theta \, P_\nu^{-\mu\,'}(\cos \Theta)$$

$$= - (\psi')^{-\mu+1} \, J_\mu'\,(\psi) \left[1 + 0(\sin^2 \tfrac{1}{2}\Theta) \right] \tag{D.6}$$

If μ is the non-negative integer m we find from Eqs. (D.5) and (D.6)

$$P_\nu^m(\cos \Theta) = \{-(\nu+\tfrac{1}{2}) \cos \tfrac{1}{2}\Theta\}^m \cdot J_m \{(2\nu +1) \sin \tfrac{1}{2}\Theta\} \left[1+0\{(\sin \tfrac{1}{2}\Theta)^2\} \right] \tag{D.7}$$

and

$$\frac{d}{d\Theta} \, P_\nu^m(\cos \Theta) = - \sin \Theta \cdot P_\nu^{m\,'}(\cos \Theta)$$

$$= -\{-(\nu+\tfrac{1}{2})\cos \tfrac{1}{2}\Theta\}^{m+1} \, J_m'\{(2\nu+1) \sin \tfrac{1}{2}\Theta\} \left[1+0(\sin^2 \tfrac{1}{2}\Theta) \right] \tag{D.8}$$
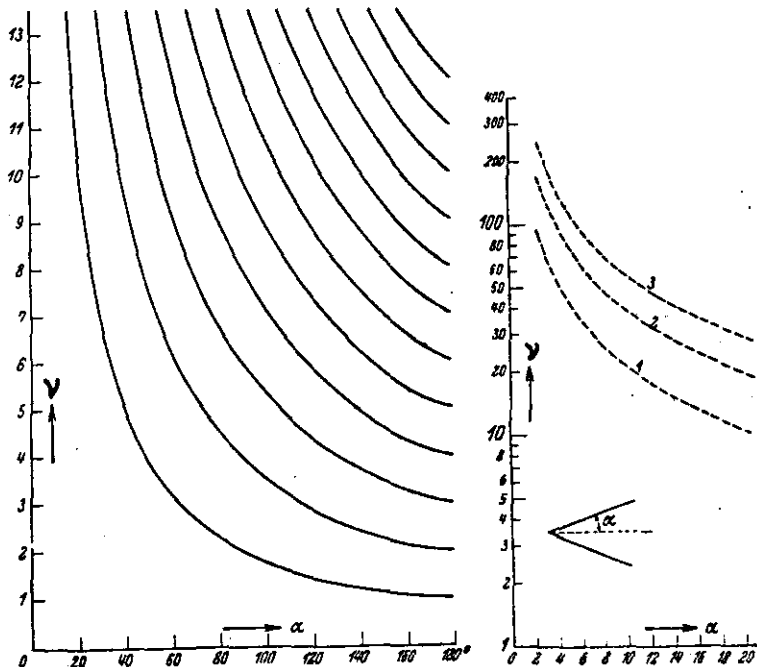

Fig. D2

The zero-points of $P_\nu^1(\cos \alpha)$: $\nu_{1,n}$; n=1,2,3,...

Eqs. (D.7) and (D.8) hold for small Θ and large ν. These requirements
are met in Chapter 2 as for cones with small $\Theta_{max} = \alpha$, ν automatically
becomes large (Eqs. (2.94) and (2.95)).
The zero-points of the function P_ν^{-1} (cos α) are graphically given
in Fig. D2, in accordance with Bucholtz (ref. 4). From Eq. (D.3) it
can be seen that these zero-points are equivalent for P_ν^1 (cos α).
Some further examples of Legendre functions are given in Figs. D3 and
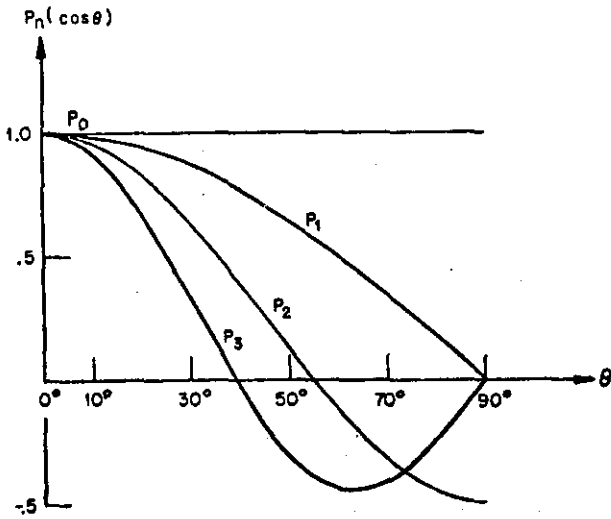D4, viz. P_n^0 (x) = P_n (x) and P_n^1 (x) for n = 1, 2, 3 and x = cos Θ.
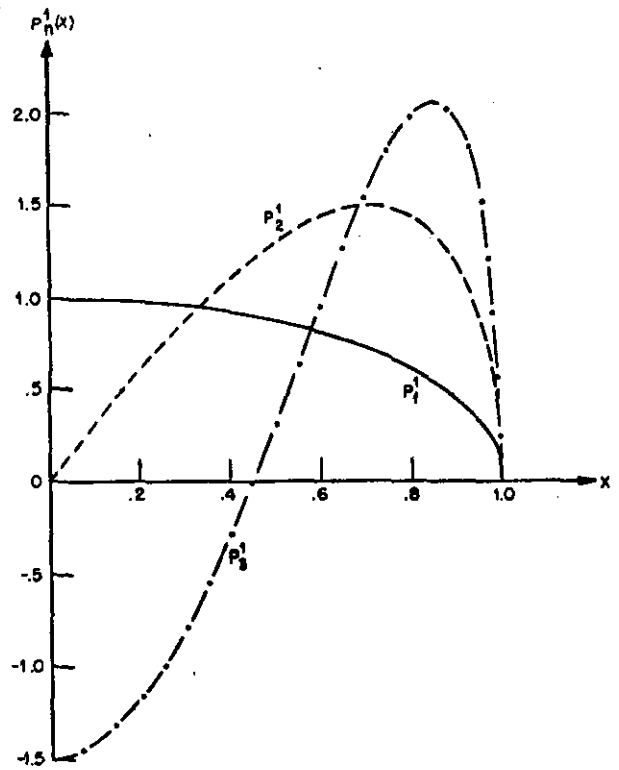

Fig. D3
P_n(cos Θ).

Fig. D4
P_n^1(x).

3. Approximations of associated Legendre functions for small Θ.

Putting x = cos Θ into Eq. (D.1) we obtain:

$$\sin^2\Theta \frac{d^2 w}{d\Theta^2} + \sin\Theta \cos\Theta \frac{dw}{d\Theta} + \left[\nu(\nu+1) \sin^2\Theta - \mu^2\right] w = 0 \qquad (D.9)$$

For small values of θ, $\sin \theta = \theta$ and $\cos \theta = 1$; other approximations are

$$\sin^2 \theta = \theta^2 \left[1 - \frac{1}{3} \theta^2 + \frac{2\theta^4}{45} - \ldots \right] \approx \theta^2$$

$$\sin \theta \cos \theta = \theta \left[1 - \frac{2}{3} \theta^2 + \frac{2}{15} \theta^4 - \ldots \right] \approx \theta \qquad (D.10)$$

Then the result is

$$\theta^2 \frac{d^2 w}{d\theta^2} + \theta \frac{dw}{d\theta} + \left[\nu(\nu+1) \theta^2 - \mu^2 \right] w = 0, \qquad (D.11)$$

where $w = f(\theta)$.

If we make the substitution $\eta = \theta \sqrt{\nu(\nu+1)}$, the equation becomes

$$\eta^2 \frac{d^2 w}{d\eta^2} + \eta \frac{dw}{d\eta} + \left[\eta^2 - \mu^2 \right] w = 0. \qquad (D.12)$$

This equation is known as the Bessel equation (Appendix C) of integer order for cylindrical polar coordinates with $B_\mu(\eta)$ as an arbitrary solution. Therefore, for small values of θ, Eq. (D.1) has the solution

$$L_\nu^\mu (\cos \theta) \approx C B_\mu (\eta) , \qquad (D.13)$$

C being a constant.

Apparently

$$P_\nu^\mu (\cos \theta) \approx C J_\mu \left[\sqrt{\nu(\nu+1)} \theta \right]. \qquad (D.14)$$

The constant C can be found by comparing Eqs. (D.7) and (D.14). It is readily seen that for small values of

$$(2\nu + 1) \sin \tfrac{1}{2}\theta \approx (\nu + \tfrac{1}{2}) \theta = \nu\theta(1 + \frac{1}{2\nu})$$

and

$$\theta\sqrt{\nu(\nu + 1)} = \theta\nu\sqrt{1 + \frac{1}{\nu}} \approx \nu\theta (1 + \frac{1}{2\nu}) ,$$

as for small conical flare angles $\alpha = \theta_{max}$, ν will be large. Therefore, the constant C becomes

Fig. D5
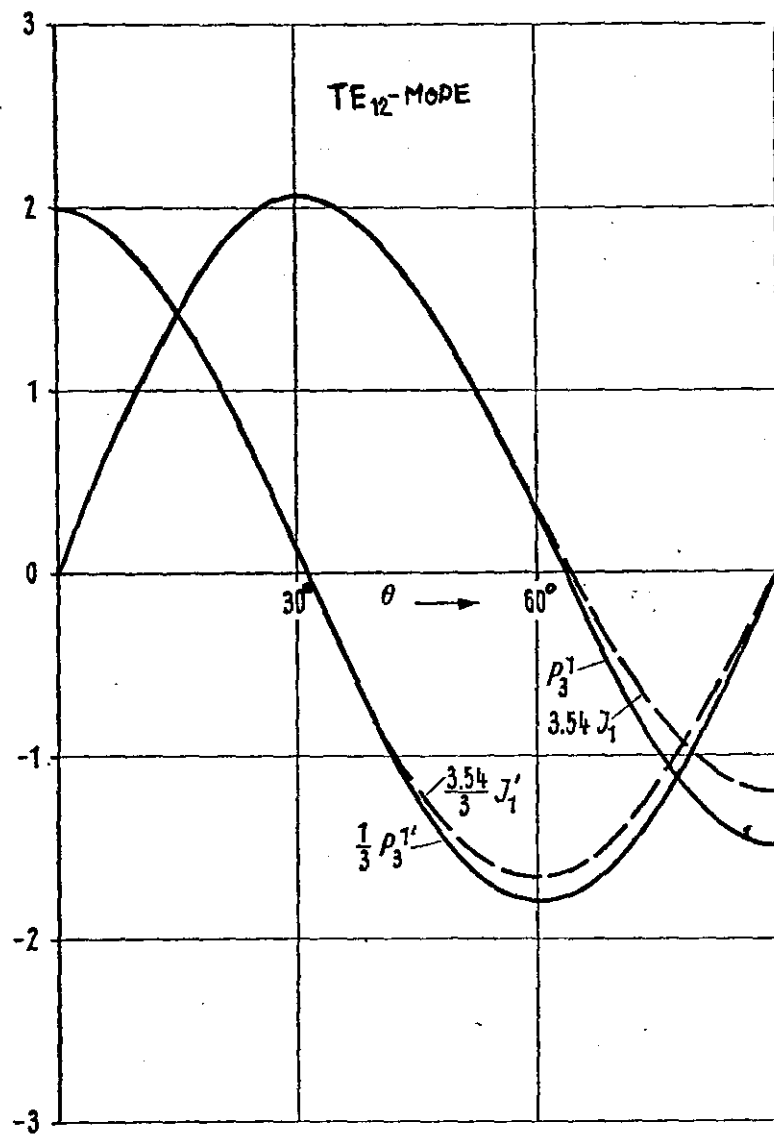
Fig. D6

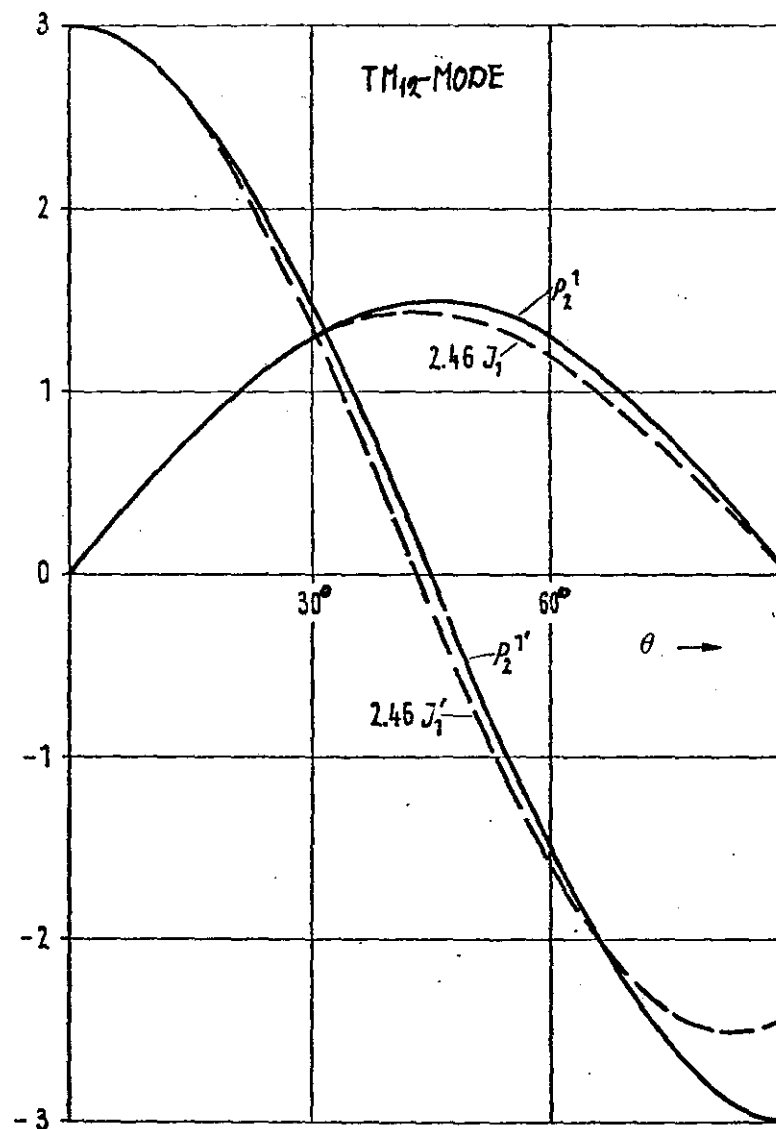Approximations of associated Legendre functions
by Bessel functions.

$$C = \left[-(\nu + \tfrac{1}{2}) \right]^{\mu + 1} \tag{D.15}$$

The equations (D.7) and (D.14) become equivalent, apart from
a coefficient.

It has been suggested that the above approximations only hold
for small values of Θ. It appears, however, that associated
Legendre functions can be approximated by Bessel functions
even for large values since $\Theta = \frac{1}{3} \pi$ (ref. 12). Piefke has
calculated that the error even for values of $\frac{1}{2}\pi$ is smaller than
1%. The Figs. D5 and D6 demonstrate the comparison between
Legendre and Bessel functions for TE_{12} and TM_{11} modes. For the
TE_{11} mode the difference between the Legendre functions and
the Bessel functions is less than 1% even for $\Theta = \frac{1}{2} \pi$.
For other modes it appears that up to a horn aperture angle
of 120° the mean deviations of the Bessel function from the
Legendre function as referred in the maximum is less than 2%.
The relative errors introduced by Eqs. (D.10) and (D.11) can,
however, become much larger.